QUEEN MARY, UNIVERSITY OF LONDON

MASTER'S THESIS 2018

Extracting neuromotor biomarkers of Parkinson's Disease from video data

---

Author:

Tanmaiyii RAO

ID : 140361229

Supervisors:

Dr. Miles HANSARD

Dr. Jonathan O'KEEFFE

M.Sc Big Data Science

School of Electronic Engineering and Computer Science

August 22, 2018

Declaration of Authorship

0.1 Disclaimer

This report, with any accompanying documentation and/or implementation, is submitted as part requirement for the degree of M.Sc Big Data Science with Industrial Experience at the University of London. It is the product of my own labour except where indicated in the text. The report may be freely copied and distributed provided the source is acknowledged.

Abstract

Tanmaiyii RAO

ID : 140361229

Extracting neuromotor biomarkers of Parkinson's Disease from video data

In this paper, methods to extract neuromotor biomarkers for Parkinson's Disease from video data have been proposed. Parkinson's Disease (PD) is a common neurodegenerative disorder that mostly affects the older population. Currently, the most common assessment for PD is by using the clinician assessed UPDRS scale. We propose a novel method for feature extraction from video data by fitting the autocorrelation function (ACF) to a damped harmonic oscillator. This method is straightforward and does not require any additional technology other than a mobile phone to record the videos. Using a more robust clinical assessment tool prevents the inter-rater variability that is prevalent for PD assessment. By using a method that detects precise features, this can enable Pd patients to have a better care. Further, classification has been done using the features achieiving an accuracy of 80% with an SVM and 75% with a Naive Bayes.

Contents

0.1 Disclaimer . . . iii

1 Introduction **1**

2 Background **3**

2.1 Overview of Parkinson's Disease . . . 3

2.1.1 Biomarkers for PD . . . 4

2.1.2 Clinical Assessment and UPDRS . . . 5

Handedness in PD . . . 7

2.1.3 Diagnosis / Treatment . . . 7

Levodopa . . . 8

Deep Brain Stimulation . . . 8

2.2 Use of Technology-based Objective Measures . . . 9

2.3 Monitoring motor symptoms using Vision based Techniques . . . 9

3 Related Work **11**

3.1 Gait Analysis . . . 11

3.2 Finger Tapping . . . 13

3.3 Other motor-symptom analysis . . . 14

3.4 Handedness . . . 15

3.5 Summary . . . 15

4 Methodology **17**

4.1 Data Collection . . . 17

4.2 Data Pre-Processing . . . 18

4.2.1 Output Format . . . 18
4.2.2 Dealing with missing Data . . . 19
4.3 Data Analysis . . . 20
4.3.1 Gait Analysis . . . 21
4.3.2 Auto-Correlation Function . . . 23
4.3.3 Finger-Tapping Analysis . . . 26
4.3.4 Feature Extraction . . . 30
Fitting a Damped Harmonic Oscillator . . . 30
Validating the model . . . 34
RMS Amplitude . . . 40
4.3.5 Classification . . . 40
SVM . . . 40
Naive Bayes . . . 42
4.3.6 Classifier Performance Evaluation . . . 43

5 Results **47**

6 Discussion **51**
6.0.1 Key Findings . . . 51
6.0.2 Limitations . . . 53
6.0.3 Future Work . . . 53
6.0.4 Summary . . . 54

7 Conclusion **55**

A Additional Plots and Tables **57**
A.0.1 Normalised Time Series Plots . . . 58
A.0.2 ACF for all subjects . . . 61

Bibliography **67**

List of Figures

4.1 a) Hand Keypoints (OpenPose, 2017a) b) Pose Keypoints (OpenPose, 2017b) 20
4.2 Scatter Plots for Right and Left Gait for a PD patient 22
4.3 Time Series Plots for Right and Left Step Speed 22
4.4 ACF for the step speed for the left and right leg of a PD patient . . . 25
4.5 Scatter Plots for Right and Left Hand for the different subjects 26
4.6 Scatter Plots for Right and Left Hand for the different subjects 27
4.7 Scatter Plots for Right and Left Hand for the different subjects 28
4.8 Scatter Plots for Right and Left Hand for the different subjects 29
4.9 a) The plot on the left depicts the curve fit for a noisy sine wave over different time lags using the fractional form as given in eq. 4.13 b) The plot on the right depicts the curve fit for a noisy sine wave over different time lags using the exponential form as given in eq. 4.12 . . 35
4.10 a) The plot on the left depicts the curve fit for the Sunspot Time series ACF wave using the fractional form as given in eq. 4.13 b) The plot on the right depicts the curve fit for Sunspot Time series ACF using the exponential form as given in eq. 4.12 35
4.11 Model Fitting for ACF for the different subjects. 36
4.12 Model Fitting for ACF for the different subjects 37
4.13 Model Fitting for ACF for the different subjects 38
4.14 Model Fitting for ACF for the different subjects 39

4.15 Linear separating Hyperplane with the support vectors as given in (Raschka and Mirjalili, 2017, p 138) 42
4.16 Confusion Matrix as given in (Raschka and Mirjalili, 2017, p 319) . . 44

5.1 Relationship between Dominant and Non-Dominant Hand 48
5.2 The confusion matrix for a) SVM b) Naive Bayes, where 0 denotes the left-handed class and 1 denotes the right-handed class. Further, the left-side has been assigned as the negative class and right as the positive class. It can be seen 49

A.1 Normalised Time Series for Right and Left Hand for all the subjects . 58
A.2 Normalised Time Series for Right and Left Hand for all the subjects . 59
A.3 Time Series for Right and Left Hand for all the subjects 60
A.4 ACF for the different subjects 61
A.5 ACF for the different subjects 62
A.6 ACF for the different subjects 63
A.7 ACF for the different subjects 64
A.8 ACF for the different subjects 65

List of Tables

5.1 Extracted Features for Left Hand 47
5.2 Extracted Features for Right Hand 48
5.3 Classifier Results 49

Chapter 1

Introduction

Parkinson's Disease (PD) is a common neurological disease affecting the elderly. This project is an exploratory data analysis (EDA) using videos of Parkinson's patients and healthy subjects. The videos have been recorded using a mobile phone camera. The gait movements of the patients have been analysed and a detailed review for not using this data for the evaluation process has been discussed. Another common way to track the motor-related symptoms for Parkinson's Disease is the finger-tapping test. Healthy subjects have been recorded doing the finger-tapping test for both hands. This has been used to identify the handedness by observing the signals in both the hands. This evaluation can be applied to PD patients to characterise their handedness and how the dominant side relates to the symptoms. The methodology used can also be applied to classify PD patients into control and interventional groups on measuring the tap amplitude and tapping frequency.

The primary aim is in the implementation of computer vision, signal processing and machine learning techniques to analyse the symptoms concerning the motor function for PD. The approaches for gait and finger-tapping assessment have been detailed in the methodology. Background and Related work focused on the application of vision and machine learning for hand tracking and gait analysis for Parkinson's disease have been included in the literature review. Further, work focused on detecting handedness using machine vision and signal processing techniques has

also been included. .

The classification experiments using the simulated finger-tapping data has been summarized in the evaluation and results section. Finally, a comprehensive critique of this approach has been outlined in the discussion section.

The main research objective is to find meaningful features to assess the motor symptoms of Parkinson's Disease (PD). The hand dominance has been used as a test case to evaluate the feature extraction process.

This project has been done in collaboration with Machine Medicine, a heath-tech startup working on detecting biomarkers from video-data.

Chapter 2

Background

This section covers the basic concepts and developments in Parkinson's Disease(PD) and the reasons for using computer vision for monitoring PD symptoms.

2.1 Overview of Parkinson's Disease

Parkinson's disease (PD) 'is the second most common neurological disorder' that affects 1–2 per 1000 of the population at any time. As the age increases, PD becomes more prevalent. It mostly affects people aged 60 and above, precisely by 1% (Miller and O'Callaghan, 2015, p 2, Tysnes and Storstein, 2017, p 901).Over 10 million people globally have been diagnosed with PD. The total cost of PD that includes treatment and other indirect expenses is approximately $25 billion per year in USA alone. On average, expenses for medications cost $2,500 annually and the cost for a therapeutic surgery per person can go up to $100,000 (Parkinson's Foundation, 2018b). PD is identified by numerous motor and non-motor symptoms that can cause a variable effect to the body functionality. The motor symptoms are more commonly visible and these mainly include bradykinesia, rigidity, tremor and impairment in 'postural reflexes'(Jankovic, 2008, p 368). Bradykinesia refers to 'slowness of movement' where the other symptoms - tremor and rigidity can be the contributors to bradykinesia but fail to explain it overall as summarized by (Berardelli et al.,

2001, p 2131). Gait instability and falling are the mainly caused by decay in postural reflexes (Bloem, 1992). Whereas, some of the non-motor symptoms are 'cognitive abnormalities, automatic dysfunction and sleep disorders' (Jankovic, 2008, p 368). However, these symptoms show up at a later stage after degenerating a large proportion of nigrostriatal dopaminergic neurons. Therefore, identifying and developing therapies that could inhibit the disease is difficult as treatment is 'symptomatic'. This also poses a massive hurdle on the healthcare system to provide effective care for PD patients. This can only be achieved via earlier diagnosis of the disease by identification of validated early biomarkers (Sharma et al., 2013, pp 201-202).

2.1.1 Biomarkers for PD

Biomarkers are measurable features that can be used as an indicator for a 'normal biological process' (Michell et al., 2004, p 1693).They can be used as criterion for the evaluation of disease progression or the treatment effects. As such, biomarkers can enable early diagnosis and provide appropriate treatment. PD biomarkers could be grouped into 'clinical, neuroimaging, biochemical, genetic or proteomic' (Sharma et al., 2013, pp 201-203). The clinical biomarkers include the observable markers or the motor symptoms such as body tremors, rigidity, etc (Sharma et al., 2013, p 206).Whereas, the neuro-imaging biomarkers include 'single-photon emission computed tomography (SPECT)' and PET that can observe the decrease in the functioning of the neurotransmitter (.)Michell2004 Another benefit of using imaging markers is that it helps to specifically identify the actual PD patients amongst all the symptomatic patients (Michell et al., 2004, p 1697). The reason being PD is one of the conditions amongst multiple disorders underlying the neurological syndrome - Parkinsonism (Psm). Psm comprises all the motor symptoms experienced by sufferers of PD although not all Psm conditions take a neuro-degenerative shape like as PD.

Further, within PD, there are varying degrees and types depending on the stage of the disease. Thus, it is essential to develop a biomarker that can differentiate the different conditions. During clinical trials, patients are given a a very powerful drug that applies to a minority of the trial participants , where the majority might not necessarily require that specific drug. In turn, leading to an ineffective diagnosis and treatment. Given these various factors, drug trials for different variants can be very expensive. To ensure proper care and management of PD patients, clinical practitioners make crucial decisions based on biomarkers (Schlossmacher and Mollenhauer, 2010). It is extremely important to identify the markers at an earlier stage, for two main reasons - to thwart the disease at the beginning itself. Secondly, to keep track of the progress of the neuroprotective therapy. As previously mentioned, if therapy is started late maybe be unsuccessful (Miller and O'Callaghan, 2015) Despite groundbreaking developments, biomarker (or a group of markers) that is uncomplicated, validated and cost-effective that can be detected at the earlier stages is not yet available (Sharma et al., 2013). The PPMI was set up to identify potential biomarkers for PD. The 'Parkinson's Progression Markers Initiative' (PPMI) is a research milestone that supports new innovations ranging from imaging to biological discoveries in detecting biomarkers for PD (Parkinson's Progression Markers Initiative, 2018).

2.1.2 Clinical Assessment and UPDRS

Despite many biomarkers, diagnosing PD is mostly based on clinical assessment where a live examination is conducted by the practitioner based on several criteria that mostly identify motor symptoms and include questionnaires about the patients lifestyle (Miller and O'Callaghan, 2015). Rating based systems are used to conduct this job and some of the common rating scales are the Hoehn and Yahr Scale and the UPDRS (Unified Parkinson's Disease Rating Scale). The Hoehn and Yahr stages is used to assess the different stages of the disease by observing the motor symptoms.

It has a scale between 1-5 with 5 being severe. The UPDRS is a more comprehensive tool that includes assessing motor symptoms e.g tremor and non-motor symptoms e.g. cognitive impairment (Parkinson's Foundation, 2018a). It is also the most widely used rating scale and it is considered the gold standard for PD assessment (Ebersbach et al., 2006, p iv32). MDS-UPDRS, sponsored by the Movement Disorder Society (MDS) is the revised version of the UPDRS that explains some of the ambiguities in the original rating system (Goetz et al., 2008). It is comprised of four sections that are as stated in (Goetz et al., 2008):

1. Non-Motor Experiences of Daily Living
2. Motor Experiences of Daily Living
3. Motor Examination
4. Motor Complications

The MDS-UPDRS measurement as given in (Goetz et al., 2008) provides a detailed approach on the way to carry out the process. Section 1, 3 and 4 need to be filled out by the examiner whilst section 2 is filled out by the patient or the caregiver. Each question has to be rated between 0-4 where 0 implies normal, 1 slight, 2 mild, 3 moderate and 4 being severe.

As this project is mainly focused on the motor features, only the motor section of the MDS-UPDRS has been touched upon. There are multiple tests to evaluate the motor section which include rigidity, finger tapping, gait, hand supination-pronation, toe tapping, leg agility, tremor, postural stability, etc. However, only the tests for finger-tapping and gait have been described as the primary analysis of this project has been on these.

- Finger-Tapping Test : The subject is asked to tap the index finger and the thumb as fast and big as he/she can. Each hand is measured independently. This test is used to assess the amplitude, speed, pauses, and decay in amplitude (Goetz et al., 2008, p 2130).

- Gait Test : The patient is asked to walk away from and towards the assessor to observe both sides of the body at the same time. The minimum walk should be 10 metre , and then turn around and walk back. The gait evaluates several factors such as stride length, speed, height of the foot lift, strike of heel whilst walking and arm swing (Goetz et al., 2008, p 2161)

Handedness in PD

Handedness or hand dominance is connected to brain asymmetry (H. Liu et al., 2009). Usually, PD symptoms have considerable asymmetry from inception (Djaldetti, Ziv, and Melamed, 2006). It is found that PD symptoms appear more often on the dominant hand-side, which is aligned with their handedness (Shi, J. Liu, and Qu, 2014). More research could be done in finding the association between dominant side of symptoms and handedness. Finding this link could help ascertain whether prior handedness is present before symptoms appear (van der Hoorn et al., 2011). As per a study done by (Barrett et al., 2011), it is found that patients who had an onset of symptoms on their dominant side, had bradykinesia than the ones who had an initial onset on their non-dominant side. Moreoever, the dominant-side symptom patients had a diagnosis and were on medication at a later stage than the non-dominant side symptom patients. Although, the severity of the disease is not affected by this , as confirmed by the UPDRS scores excluding the subscore focusing on dominant hand tasks. However, this can be very useful in assessing the early signs and the period between diagnosis and starting dopaminergic treatment (Barrett et al., 2011).

2.1.3 Diagnosis / Treatment

There is no permanent cure for PD as such yet, although the disease progression can be slowed down (Goetz, 2011). Some of the most common treatments for PD

depending on the stages are as follows :

Levodopa

LevoDopa (L-Dopa) is a typical initial dopaminergic treatment for PD. It is very effective in reducing the motor symptoms such as bradykinesia, tremor and rigidity. Although, as the condition becomes worse, other motor problems start developing such as posture imbalance and freezing of gait. L-Dopa is usually ineffective when treating the latter advanced symptoms (Fahn, 2018, p S2). Another issue is that with continued usage , majority of patients suffer from drug-induced dyskinesias(involuntary movements) and other motor problems. Other medicines are used to treat these symptoms (Jankovic and Stacy, 2007, pp 678-679).

Deep Brain Stimulation

When L-Dopa becomes less effective in the advanced stages, Deep Brain Stimulation (DBS) could be performed. DBS is a surgery that is only recommended for PD patients who have been living with the condition for a minimum of 4 years where the side-effects of L-Dopa become evident. A thorough assessment is conducted to assess whether the patient can undergo DBS. The procedure involves placing electrodes (thin wires) into either the left/right or both parts of the brain in particular regions that 'control movement'. DBS is effective in motor symptom reduction such as slowness, tremor and stiffness. Although it is not so effective in lessening non-motor symptoms and imbalance (The Michael J. Fox Foundation, 2018).

There are other types of treatments which are not covered in here.

2.2 Use of Technology-based Objective Measures

Conventional measures like the UPDRS can cause intra-variability (at different times)(use ref) and inter-variability when the same patient being assessed by different examiners (Pal and Goetz, 2013). Relying fully on the judgment of clinical practitioners who are not exempt from making occasional diagnostic errors, can hinder advances in research (Miller and O'Callaghan, 2015). In the last decade, there has been a rise in the use of technology-based objective measures (TOMs) used largely for motor symptoms such as step/ tapping frequency and amplitude. TOMs range from wearable sensors, mobile applications, videos, etc. However, the TOMs that are mostly used are wearable sensors such as accelerometers, magnetometers and gyroscopes (Espay et al., 2016). Sensors improve accuracy and sensitivity and can be useful in minimizing the inter-rater variability. Further, they may also help in estimating the treatment effects for the motor symptoms which could be not be so evident during initial stages of the disease (Pal and Goetz, 2013). As such wearable sensors could be used for monitoring patients remotely as well. Although, the data collected in remote settings might not always give accurate information for instance it cannot be inferred from sensor data alone whether movement slowness picked up by the sensor is a result of bradykinesia or fatigue. Moreover, subjects could face discomfort and be unwilling to be using these devices on a long-term basis (Espay et al., 2016).

2.3 Monitoring motor symptoms using Vision based Techniques

Monitoring via video-based metrics eliminates the shortcomings of using wearable sensors. Also, with using a video footage, the examiner can always refer to the video to validate the scores. Further, motor function measures such as step frequency for gait, tapping frequency for finger-tapping and amplitude can be extracted from the

videos. This is possible through applying computer vision, machine learning and signal processing techniques.

Computer vision techniques are being applied in medical imaging for 'Human Activity Recognition(HAR)' and fall detection to name a few. Further, machine learning and deep learning techniques that use deep neural networks have been implemented to extract features from the images and videos (Gao et al., 2018). Artificial Intelligence is transforming healthcare. The rise of deep learning and computational power (GPUs) have made this possible. This could be applied to monitoring PD motor symptoms (Lancet, 2017). One such method is by doing pose estimation for the subject in the video. Pose estimation algorithms can be implemented by using computer vision, machine/deep learning techniques. In this project, OpenPose has been used, that uses a Convolutional Neural Network(CNN) to extract the pose (Cao et al., 2017, Simon et al., 2017, Wei et al., 2016). From the pose metrics, the frequency and amplitude can be derived using signal processing techniques. Lastly, the metrics can be used to do a classify the subjects into different groups based on the stage of disease progression.Supervised learning methods could be used in the cases of labelled data (Jordan and T. Mitchell, 2015). The main approach is detailed in the methodology and similar methods are described in the Related Work section.

As mentioned earlier, the cost of clinical trials for PD is very high due to the lack of validated biomarkers (Schlossmacher and Mollenhauer, 2010). Using vision-based markers can give a precise result and eliminate the bias of just relying on clinicians judgment. A study done by (Artusi et al., 2018), found that clinical trials using TOMs comprised of only 2.7% amongst which more than 75% constituted sensor-based markers (Artusi et al., 2018). This shows that vision-based markers are not widely used for PD assessment. Given, the video is taken in suitable conditions (considering the camera angle, avoiding disturbances, and having the entire person in the frame). Validated metrics can be potentially extracted from the video that can assess the motor function and differentiate the patient groups.

Chapter 3

Related Work

This section gives an overview of previous research in PD focused on gait analysis and finger tapping which includes different methods using computer vision, sensors, machine learning, deep learning and others. Also, previous work for other motor symptoms has also been included. Research related to gait and handedness that is not characterised by PD has also been talked about. Since, the research idea could be potentially applied to any condition. This section shows that the scope of simple implementations using computer vision is still limited.

3.1 Gait Analysis

Most methods to analyse gait use sensors as previously discussed. These include micro-intertial sensors, pressure insoles and wireless surface electromyography. Although, the time and cost it takes for setup can inhibit the use on a large scale (Wong et al., 2015). Further , other methods using computer vision , cameras have been suggested to extract gait metrics such as step length, ground reaction force(GRF) and angle of foot. However, these have similar problems as sensors in term of complexities in configuring the apparatus (Deligianni et al., 2018, p 260). Moreover, most vision-based systems use multi camera system , not a single RGB camera (Deligianni

et al., 2018). Thus, using a single camera, would be more convenient and easily accessible in the real environment. (Gu et al., 2018) propose a markerless vision-based tracking system that uses one RGB camera for the estimation of 3D angular parameters of the lower limbs. OpenPose has been used to extract the 2D joint coordinates combined with GrabCut to detect the foot position. Followed by a 3D reconstruction using an active shape model (ASM) and sparse dictionary methods. Finally, the gait metrics from the 3D space have been extracted such as foot progression angle and 3D foot-leg angle. These angles can be used to measure dorsiflexion/planarfelxion and inversion/eversion angles. Since, these angles can be used to diagnose gait abnormalities in elderly patients and the ones suffering from neurological disorders like PD (Gu et al., 2018, pp 42-43).

(Cho et al., 2009) have proposed a vision framework to identify the gait features in PD and classify subjects into healthy controls and PD patients. Both, Principal Component Analysis (PCA) and Linear Discriminant Analysis (LDA) have been used to extract the metrics. This is implemented by the algorithm by preprocessing the video into a series of images comprising the gait movements of the 'human silhouettes' from the video (Cho et al., 2009). This system has been improved by (Chen et al., 2012) to also include the UPDRS scores to ascertain the abnormality level by implementing a regression algorithm that predicts the UPDRS score for gait from the image sequences, as well as classifying subjects into healthy control and PD patients that uses LDA (Chen et al., 2012).

(Ťupa et al., 2015) have used MS Kinect to collect gait data from PD patients and healthy controls. MS Kinect is a depth sensor that has two components - an infrared camera and an infrared projector. A skeleton algorithm that extracts the the coordinates from the skeleton in a 3D space has been implemented for the collected data. Using the points, the leg length, stride length (SL) and the gait velocity (GV) have been extracted. Further, the subjects have been classified into control and patients using an Artificial Neural Network (ANN) based on the extracted gait features

(Ťupa et al., 2015).

Other studies focused on identifying Pd patients from healthy controls mostly use sensor data. (Medeiros et al., 2016) use public sensor data for VGRF (vertical ground-reaction force) to classify gait impairments by implementing a PCA algorithms. (Baby, Saji, and C. S. Kumar, 2017) uses sensor data from PhysioBank, to classify PD patients based on their gait characteristics. Wavelet transforms have been used to extract the features. Patients and healthy subjects have been classified using an ANN and have been compared with other classifiers such as Support Vector Machine (SVM) and Naive Bayes. It is found that ANN gives the best accuracy. This could be due to the use of backpropagation in neural networks which are not present in simple ML classifers (Baby, Saji, and C. S. Kumar, 2017).

3.2 Finger Tapping

Similarly, prior research for finger-tapping analysis has mostly extracted features from sensors or by setting up a system in predefined conditions. (Martinez-Manzanera et al., 2016) use a 9 degrees of freedom (DOF) sensor to detect finger-tapping and toe-tapping movements. Using the time series signals from the data, the relevant features have been extracted. These parameters have been incorporated in an SVM to automatically score the tapping movements for each patient emulating the UPDRS scores (Martinez-Manzanera et al., 2016).Although this bridges the gap for inter-rater variability, using sensors can cause discomfort and it is not non-invasive.

Whereas, (Lainscsek et al., 2012) use a motion capture system consisting of 12 cameras and IRED markers placed on the subjects to track the finger-tapping movements. A model based on non-linear delay differential equations (DDE) has been proposed to classify the patient and control groups. The DDE has been fitted to the time series (of both groups) using a genetic algorithm where the co-efficient of the DDE is used to detect the severity of motor dysfunction. The model was strongly

correlated ($0.785, p < 0.0015$)with the UPDRS scores that suggests the model is affirmative (Lainscsek et al., 2012). Despite showing good results, the difficulties in setting up the system to capture data , inhibit the widespread usage (Wong et al., 2015).

On the other hand, (Khan et al., 2014) have proposed a vision based model to capture the finger-tapping movements from a video by normalising the amplitude/distance by the face. The tapping movements are detected by using a motion template-gradient algorithm that detects the change in pixel locations across the time frames for the required points in the video i.e the index-finger movement. Additionally, Haar Cascade Classifier has been used to detect the face and in turn, normalise the distance by the face distance. This was applied since subjects were asked to place their hands next to the face on both sides whilst doing the rapid finger-tapping test. Once, the finger-tapping time series have been computed, metrics such as tapping speed, amplitude and rhythm have been extracted using a peak-finding algorithm. Lastly, the features have been used to train an SVM to classify the patient and control groups. Further the classifier has also been used to separate the patients based on their UPDRS scores by collating the model with prior UPDRS scores (Khan et al., 2014). Compared to previous models, this model is the easiest to implement in daily-environment. Although, placing the hand next to the face can be problematic if the patient has severe PD, as they would be unable to lift their hand with ease.

3.3 Other motor-symptom analysis

(M. Li et al., 2017) have used Convolutional Pose Machines(CPM) to differentiate between PD patients and patients with Levodopa-Induced Dyskinesia(LID). CPM is a deep learning technique implementing a CNN, to do a pose estimation (PE) on the video data. It is a precursor to OpenPose, and has been implemented by the same group of researchers that developed OpenPose (Wei et al., 2016,Simon et

al., 2017,Cao et al., 2017). The motor function metrics such as frequency have been extracted from the PE output points using spectral analysis. Communication and Drinking tasks have been used to capture data from LID patients. Whereas, toe-tapping and leg agility have been used for PD patients. Finally, a binary classification has been done using the extracted features to identify the two different groups (M. Li et al., 2017).

3.4 Handedness

When it comes to handedness, prior research in classifying hand dominance has been done using the test for finger tapping. (Hubel et al., 2013) use a 'computerized finger-tapping test' in which subjects were asked to press a button on a gaming mouse with the index finger while placing the palm on top of the table. The tapping was done for a 10 seconds and on both hands. It was found that there was a noticeable distinction between the dominant and non-dominant hand for the rate of tapping, decay in tapping, and the initial-tap time and after-tap time (Hubel et al., 2013). Similarly, (Aoki, Rivlis, and Schieber, 2016) have used different gestures using the index finger to measure hand asymmetries for dominant and non-dominant hand using the touchscreen on an iPod Touch (Aoki, Rivlis, and Schieber, 2016). There has not been prior research done in using computer vision frameworks to extract features to measure hand dominance. It is still an area that needs to be explored. In this project, by using OpenPose, it is evaluated whether relevant features can be extracted accurately to classify the dominant hand from finger-tapping.

3.5 Summary

Although, novel approaches have been developed, a method that is non-invasive and easy to implement is yet to be developed. Despite, their good accuracy scores,

the above methods can be obtrusive to implement on a wide-scale in a clinical set-up. The benefit of implementing a PE algorithm like a CPM or OpenPose (OP) is that numerous features can be extracted in fewer stages using the extracted pose output points. This makes it scalable to be integrated in clinical settings. (Gu et al., 2018) point out the limitations of implementing OpenPose (OP) as it does not output data in 3D, it only captures 2D points accurately. In order, to extract simple and yet powerful metrics such as frequency (step and finger-tapping) , 2D points works as angle between foot or fingers is not being considered. In this project, OP has been used to extract the key points that has been outlined in the next section.

Chapter 4

Methodology

In this section, the main approach taken for this project is explained in depth. The following sections will explain different stages

4.1 Data Collection

The patient data has been provided by Machine Medicine. These patients were separated into two different groups - baseline (prior to the treatment) and active trial (after the treatment) (ClinicalTrials.gov, 2018). The gait data was of varying lengths and there were occlusions in the video, multiple persons, or moving gait of the person recording it. Only the videos that had a single person and were of usable quality to be put in for pose estimation have been used. Despite that, the videos failed to generate a good signal and thus have not been further analysed. The process has been explained in the remaining sections.

The finger-tapping data has been simulated from 15 healthy subjects. Each person has been recorded doing the finger-tapping test i.e to tap the index finger against the thumb for 5 secs on each hand. Subjects have been asked to place the thumb in a horizontal position parallel to the face , and the index finger perpendicular to the thumb while tapping. Whilst doing the finger-tapping, it was ensured that the entire person was in the video frame. This was essential, as the pose estimation

could only be done when OpenPose can identify a person in the frame and the different body parts. All subjects were seated on a chair and it was shot on a normal smartphone camera from a distance of 2-3ft away from the subject. The videos then were split to separate the right hand tapping and left-hand tapping before doing the pose estimation.

Amongst the thirteen persons, 3 were left-handed and the remaining 10 were right handed. The next step to get a meaningful picture of the data was to put the videos through pose estimation.

Python and MATLAB have been used for the code implementation. The initial data extraction process has been done using Python and its supporting libraries. Whilst the feature extraction process has been implemented in MATLAB.

4.2 Data Pre-Processing

OpenPose was used to extract the pose estimation from the video data. OpenPose is an opensource computer vision library used to do a pose estimation that uses deep learning methods such as convolutional neural networks (CNN) (Wei et al., 2016,Simon et al., 2017,Cao et al., 2017). It is built using C++ packages and OpenCV and Caffe are the underlying packages. By default, it is installed on a GPU system since it helps in faster execution. To process the data, an AWS GPU was used on which the OpenPose library was installed. The GPU and the library was installed on Machine Medicine's analytics server, from which the pose estimation (PE) files were downloaded.

4.2.1 Output Format

The output for the pose estimation can be saved as json files where all the body parts are saved in a dictionary format. The different pose estimates can be separated into

body, left hand, right hand and face coordinates. Each keypoint has 3 values (x, y, c) where x and y are the $2-d$ coordinates and c is the confidence interval that the points have been correctly detected.

An example output of the json which has been formatted as a jsonl object in which each line represents a timeframe with the different pose keypoints. In the current version of OpenPose can only track 2d pose estimates thus the 3d keypoint values are not detected.

The following represents the output format in one timeframe (json line) :


```
"people": [{"hand_right_keypoints_2d": [988.25, 792.564, 0.218758,.....], "hand_left_keypoints_3d": [], "pose_keypoints_3d
    ": [], "pose_keypoints_2d": [618.586, 465.536, 0.672114,.....], "face_keypoints_2d": [578.32, 552.893, 0.614508,
    .....], "hand_right_keypoints_3d": [], "hand_left_keypoints_2d": [869.082, 243.094, 0.510394,.....], "
    face_keypoints_3d": []}], "version": 1.2}
```


The keypoint listing for the pose output and hand output has been has been given in figures 4.1 and 4.1. The keypoints for the gait points are $1, 8, 9, 10, 11, 12, 13$ comprising the center of the shoulder , the hip, knee and ankle points for the left and right legs respectively. For the finger tapping, points 8 and 4 have been extracted for both left and right hands.

4.2.2 Dealing with missing Data

Quite often, there are missing frames, in which the pose output would be an empty list or return null values. Such frames have been discarded if there are more than 7 consecutive frames with missing values. If it is less than 7 frames, the missing data has been estimated using linear interpolation. Interpolation is a common method to predict values between a certain range.

If there is a function $y = f(x)$ where $y1 = f(x1)$ and $y2 = f(x2)$ when $x1 < x2$. This is used to estimate the value of $f(x)$ when $x \in (x1, x2)$. When it is assumed that that is a linear relationship with $f(x) \in [x1, x2]$, the technique is called linear interpolation. This is one of the most common interpolation techniques to fill in missing data

and is determined in the following way (Pownuk and Kreinovich, 2017, p 1):

$$f(x) = \frac{x - x1}{x2 - x2} \cdot f(x2) + \frac{x2 - x}{x2 - x1} \cdot f(x1) \tag{4.1}$$

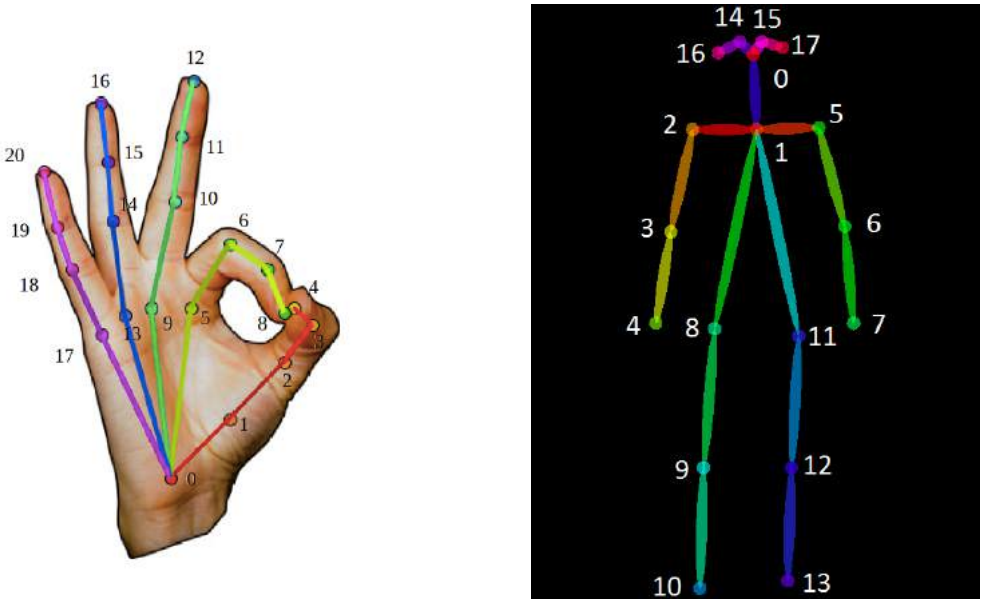

FIGURE 4.1: a) Hand Keypoints (OpenPose, 2017a) b) Pose Keypoints (OpenPose, 2017b)

4.3 Data Analysis

After all the required data has been pre-processed, the next step was to extract the time series for the gait and finger-tapping. From the time series data, some of the motor assessments from the UPDRS such as the step frequency , tapping frequency and the decay (how fast the stride length or amplitude) decreases (Goetz et al., 2008). Firstly, gait analysis has been done on sample data and the explanations for not proceeding with this has been outlined. Followed by the analysis for finger-tapping.

4.3.1 Gait Analysis

To analyse gait for PD, the patient is asked to walk away and towards the examiner covering atleast 30 feet. This implies to walk from the point where the examiner is , and walk back to the same starting point. Essentially, this means that whilst the person is walking away, the person's back is visible to the examiner and vice versa will walking towards the camera.In most of the videos, the subject is seen walking sideways in front of the examiner where the right gait is visible while walking away and the left gait when walking back. When you have a view of both the legs, it is easier to interpret both together (Goetz et al., 2008). Doing pose estimation on these videos would not be a problem as the step frequency can be estimated separately for the left leg and right leg using the specific keypoints. Although, more than often, the pose estimation has not been done for many consecutive frames, as sometimes the face of the person is missing with a focus on the legs. Other times, there have been occlusions in the scene where there is a wall, or walking between two rooms. Also, when there are multiple persons, to only extract the points for the subject.

Given, the time scale for the project, the gait analysis was beyond the scope of this project. As it would have required a lot more pre-processing. First, to discard the irrelevant frames that did not have the person and to get only those parts of the video that had a good gait signal. Another, issue was that since the person is seen walking towards and backwards, the impact of turnings and pauses had to be taken into consideration. As fitting the data with these into a model could disrupt the periodic signal and can give misleading results. Due to all these reasons, the gait analysis has not been proceeded further.

However, the approach for initial analysis of gait has been included that has been analysed on a clean sample where the video has been taken accurately.

The initial steps was to first extract the necessary keypoints as given in figure 4.1 where keypoint(kp) 1 is the centre of the shoulder and kp 8 and 10 are right and left

hips respectively. The average of vectors $\left\|1\vec{\cdot}8\right\|_2$ and $\left\|1\cdot\vec{11}\right\|_2$ have been calculated to determine the center vector. Since the size of the person varies depending on the distance from the camera, the coordinates have been normalised using the center vector scale. A glimpse of the gait signal can be observed by looking at the scatter plot of the raw data (scaled according to the center vector). The x and y position of the ankle for the whole video clip has been plotted below for the left and right leg.

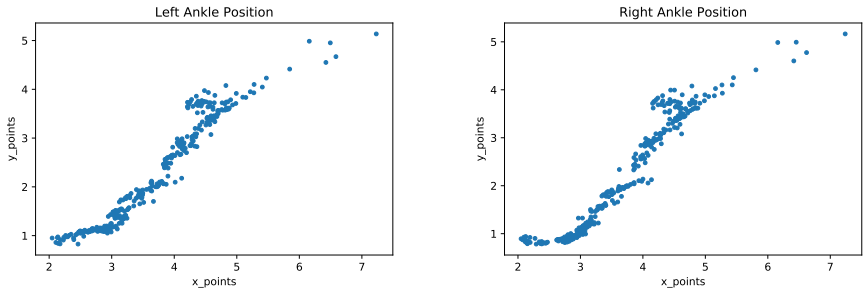

FIGURE 4.2: Scatter Plots for Right and Left Gait for a PD patient

The first derivative of the ankle point has been taken to observe the change in velocity or speed across time by taking the euclidean distance over the different time frames. t will be 1 since t cancels out when $t+1-t$. Thus the equation becomes

$$StepSpeed = \sqrt{(x_{t+1} - x_t) + y_{t+1} - y_t)} \tag{4.2}$$

The plot for the step speed is given below:

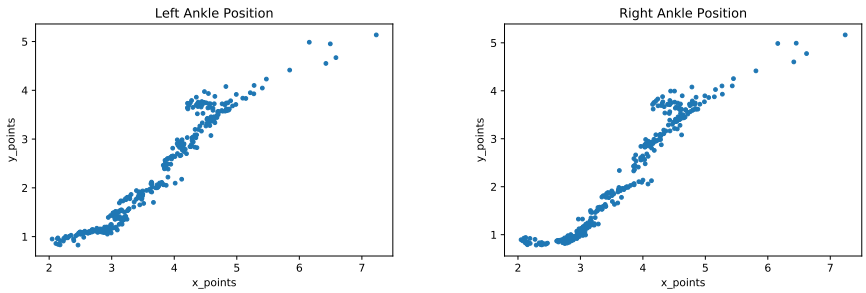

FIGURE 4.3: Time Series Plots for Right and Left Step Speed

4.3.2 Auto-Correlation Function

The next step was to observe the autocorrelation function (ACF) across time. This method has been used for both gait and for the finger-tapping data. The ACF is a pivotal technique for time series analysis. It can be defined as the correlation of the time series with itself at particular 'time steps' called lags (Rafiee and Tse, 2009, p 1558). This can be expressed as a function of the two time points where k is the lag (the difference between t+k and t). The formula for ACF for lag k is as follows (Sanborn and Ma, 2005, p 230):

$$c_k = \frac{\sum_{i=1}^{N-k}(x_i - \overline{x})(x_{i+k} - \overline{x})}{\sum_{i=1}^{N}((x_i - \overline{x})^2} \quad where -1 \leq c_k \geq -1 \tag{4.3}$$

If the time series is 'univariate' as in this case, the ACF is synonymous with the Pearson correlation co-efficient of the time series with the lagged version of itself. (Zhou, 2014, p 1) The Pearson correlation co-efficient (Pearson Product Moment) measures the linear dependency of two variables and returns a single value in the range -1 and 1 with 1. The ACF at lag 0 would always be 1 since it is perfectly correlated with the time series being alike (Nelson-Wong et al., 2009).

The general form of the Pearson Correlation Co-efficient is given by (Paradis, 2009, p 1):

$$r = \frac{\sum_{i=1}^{n}(x_i - \overline{x})(y_i - \overline{y})}{\sqrt{\sum_{i=1}^{n}((x_i - \overline{x})^2}\sqrt{\sum_{i=1}^{n}((y_i - \overline{y})^2}} \tag{4.4}$$

As such, equation 4.3 can be derived from equation 4.4 by substituting the time series values and calculating the autocorrelation at a certain lag. Although, the ACF differs from the Pearson in the sense that the Pearson product returns one value that measures the linearity between 'two variables'. Whereas the ACF is a series of Pearson r values where each $R_k(X)$ is the correlation between the original time series values and the values at each lag (Nelson-Wong et al., 2009).

The use of ACF is widespread in the fields of science , to analyse periodicity in signals and for detecting specific useful features in signal processing. ACF can also be applied to observe patterns in medicine and 'human movement science' Thus it can applied to observe gait patterns and finger-tapping movements by detecting the periodic signal within the noise (Nelson-Wong et al., 2009, p 291). Since the ACF calculates the correlation of the signal with itself, crucial features can be extracted by observing the correlation between the signal's amplitude at one time point to its amplitude at a lagged time. Also, the characteristics of the time-series signal can be determined from the ACF by observing its pattern. Despite the ACF being a linear function, it can be applied to model non-linear and non-stationary time series (Flores, Engel, and Pinto, 2012). The series would be stationary if the ACF decreases rapidly and non-stationary if the ACF wears out at a slow rate. Thus, ACF can be one of the most informative technique since the output produced have negligible variability from one signal to the other even if the raw data signals are non-stationary processes (Rafiee and Tse, 2009, pp 1566-1568). ACF can be used as an alternative to spectral analysis such as Fast Fourier Transforms (FFT) to observe the frequency. Methods like FFT work well with stationary signals which are not random whereas ACF can be applied to random processes, that can occur sometimes in the case of finger-tapping and gait if patients are suffering from severe PD (Nelson-Wong et al., 2009). Further, FFT works well , when the length of the signal is long. Otherwise it fails to capture accurate measure of the frequency (Lainscsek et al., 2012). In this project, the signal data is less than 10 seconds.

One important aspect for ACF is the lag. The number of lags used can influence the generated output. This number is dependent on the type of data and can be set by testing different values. In this case, a lag of 90 has been set by trial and error. This captures the periodicity fairly well. If the number of lags are small, it would fail to produce an accurate output whilst a very large value could be computationally more expensive (Sanborn and Ma, 2005). Although, it is generally observed that the

more lags, the better the performance (Rafiee and Tse, 2009).

Before calculating the ACF it is a good practice to normalise the data to one scale. This is to ensure that all the values are on the same scale (ref). Additionally, it is essential to detrend the signal before computing the ACF otherwise the generated output could be affected by non-zero mean and the trend components (Wu et al., 2007). This has been done using the MATLAB inbuilt function detrend to remove the linear trend. Further , the detrended signal has been smoothened using Gaussian filter to remove the random noise.

The ACF for the step speed time series for gait has been plotted below:

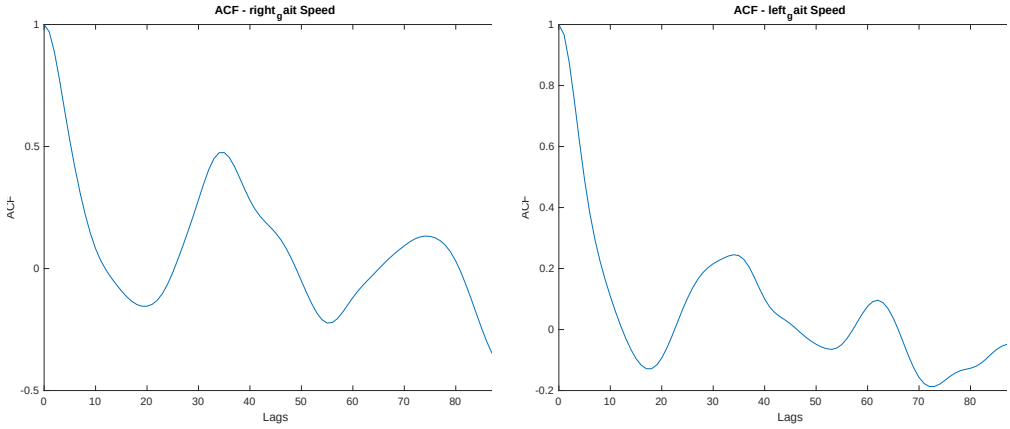

FIGURE 4.4: ACF for the step speed for the left and right leg of a PD patient

From the figure 4.4, it can be seen that periodic signal decays very fast. The reasons for this being that there have been pauses in the video where the subject stopped, during turnings to walk back. These instances can distort the periodicity of the signal. Given the time scale for the project, analysing gait and deriving meaningful features would have been beyond the scope of the project. Thus, simulated data using finger-tapping for handedness has been used as a test case to support the main hypothesis.

4.3.3 Finger-Tapping Analysis

As discussed earlier, 15 healthy subjects have been recorded doing the finger-tapping test. In the generic finger-tapping test for PD, the subject is asked to tap the index against the thumb as fast as they can and for 10 sec (Goetz et al., 2008). Unlike, the standard test, subjects in this case were asked to tap their fingers at their natural pace. To maintain consistency within the around 3-4 seconds of tapping signals have been extracted from the pose estimation for each hand from the videos. Due to the differences in camera, some videos had a frame rate of 60 fps whilst most had 30 fps and and a few with 25 fps and one with 25 fps. This implies around 240 frames and 120 frames of data have been used in the data analysis.

The first step in the finger-tapping data analysis process was to plot the raw data points. The scatter plots similar to the gait, has been depicted below for the different subjects. Only one sample for each subject has been included. The x and y position of the index finger has been observed across the entire video. To avoid confusion of the points, the x and y points have been normalised to a scale of zero mean $\mu = 0$ and standard deviation $\sigma = 1$. This is the standardisation process using z-score to normalise data. Z-score normalisation significantly reduces noise in data (Cheadle et al., 2003) :

$$d_z = \frac{d_i - \mu_{data}}{\sigma_{data}} \text{ for } d_i \in data \tag{4.5}$$

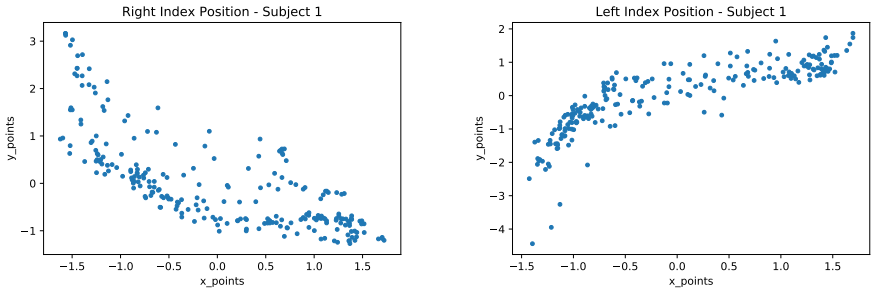

FIGURE 4.5: Scatter Plots for Right and Left Hand for the different subjects

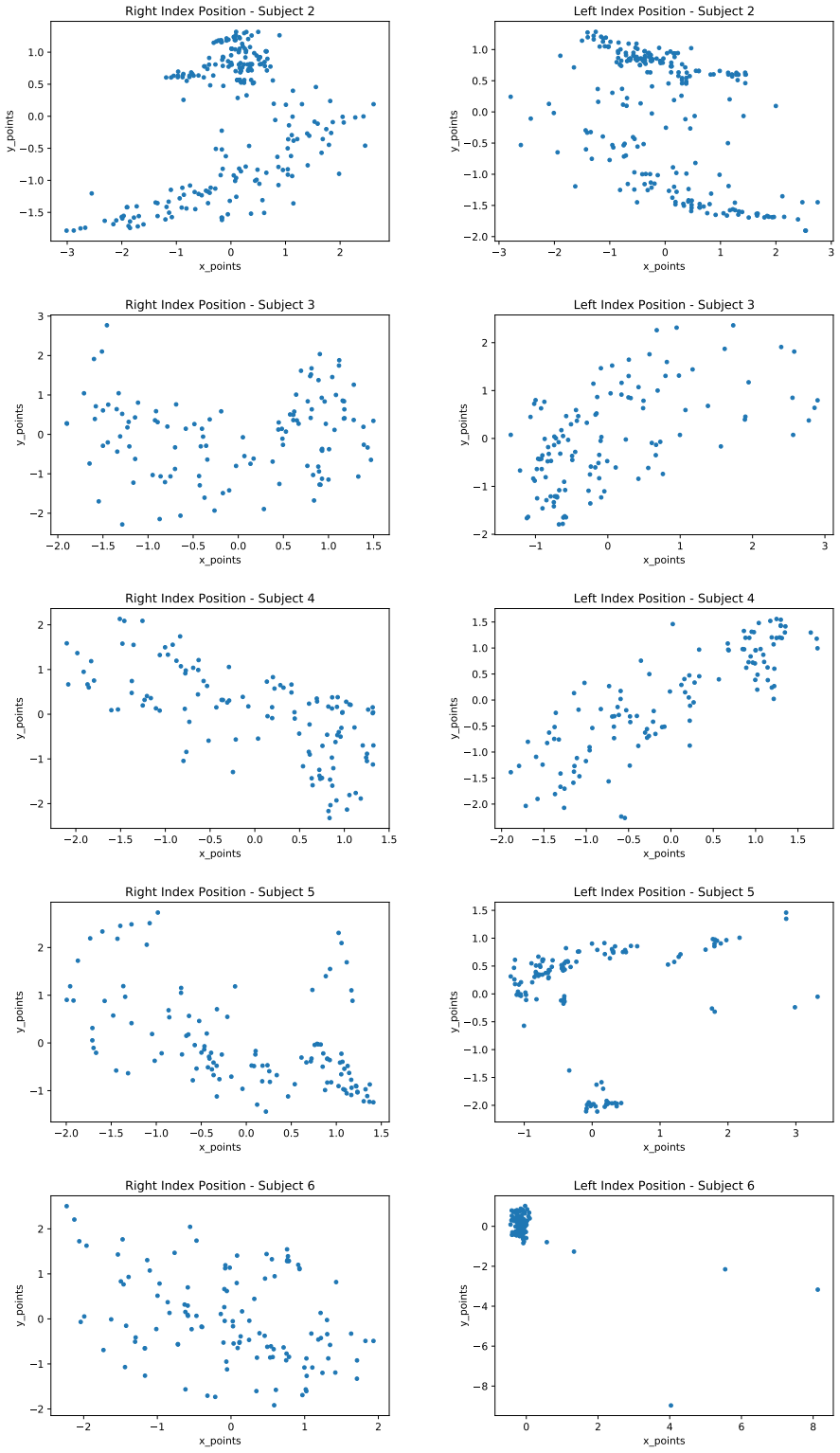

FIGURE 4.6: Scatter Plots for Right and Left Hand for the different subjects

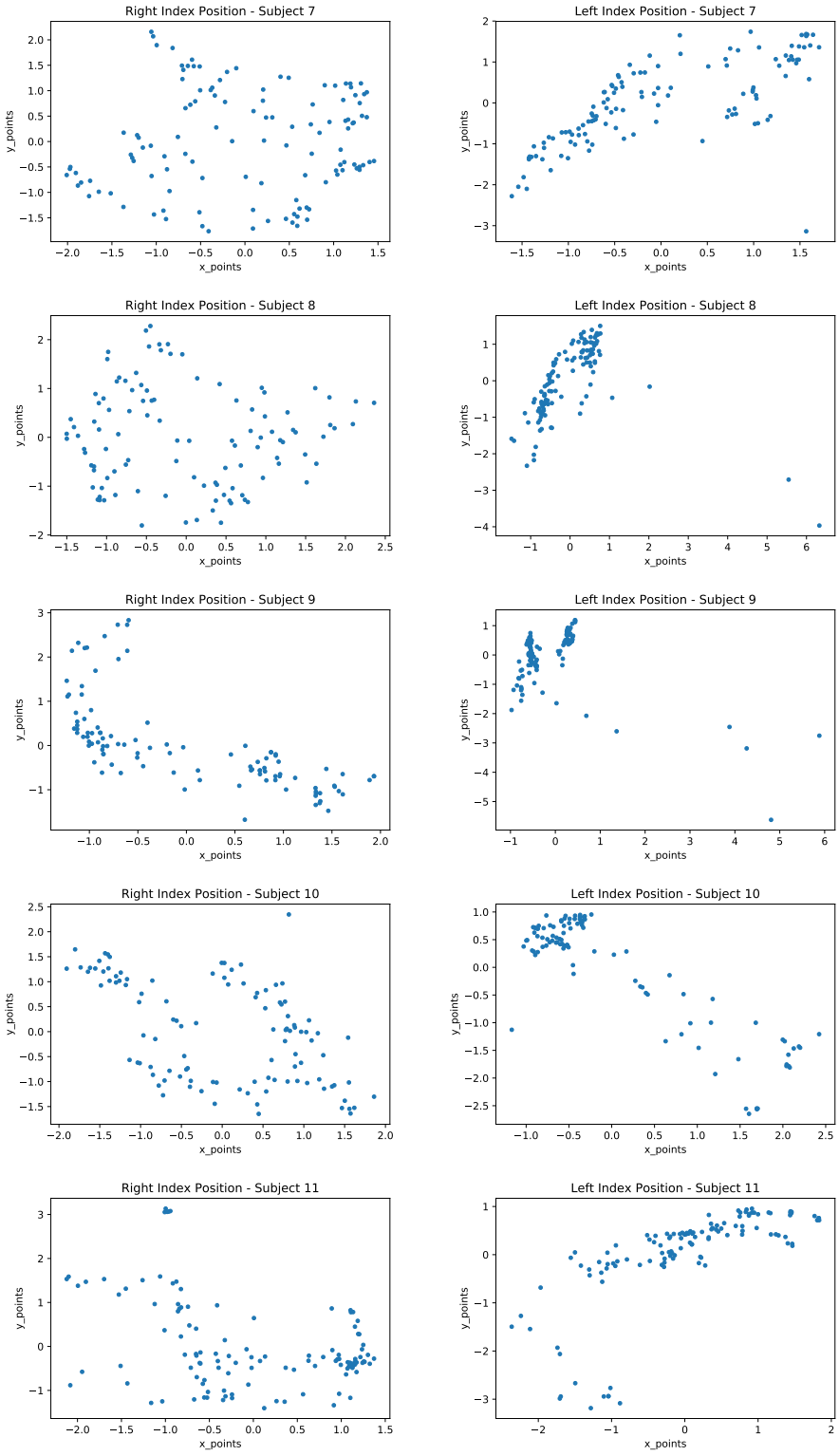

FIGURE 4.7: Scatter Plots for Right and Left Hand for the different subjects

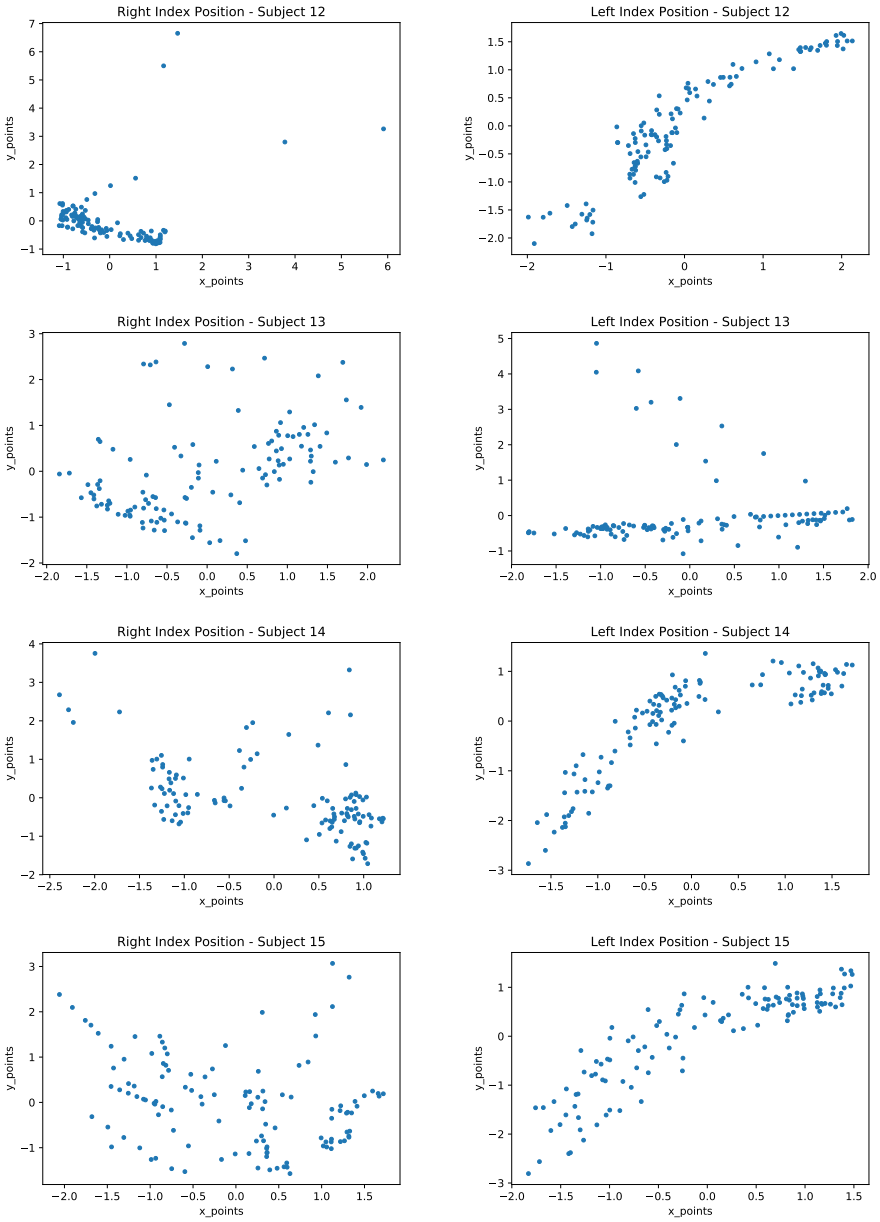

FIGURE 4.8: Scatter Plots for Right and Left Hand for the different subjects

The next step was to calculate the amplitude for each tapping and extract the amplitude time series for all the subjects. To do this, the euclidean distance between the thumb and index has been computed across all the time-frames. The plots for the distance time series have been given in figures. The distance is in pixel units. The euclidean distance in a 2-D plane is the root of squared distance. This is the formula

for calculating the Euclidean distance or L2 norm in a 2d plane (Greche et al., 2017):

$$||d||_2 = \sqrt{(x_2 - x_1^2) + (y_2 - y_1^2)} \tag{4.6}$$

In-order to keep all the data in the same scale, the distance has been normalised as per 4.5 and the plots have been given in the appendix A.

The next step was to get the autocorrelation function (ACF) that has been calculated using 4.3. The data has been normalised using 4.5 before computing the ACF. Further, the time series has been detrended to remove the trend. Followed by smoothing the data using Gaussian filters to remove the noise from the data. The plots for the ACF have been given in the appendix

4.3.4 Feature Extraction

In-order to extract the features to assess-finger tapping movements (Goetz et al., 2008), such as decreasing amplitude and tapping rate, the ACF curves are fitted into a model to extract the parameters. These correspond to a sinusoidal-cosine wave like signals with variations. Some of the ACFs have decreasing peaks or damped waves. This resonates with a damped harmonic oscillator and thus the ACF has been fitted to a damped harmonic oscillator model to extract the decay and frequency parameters. The ACF plots that have been fitted to the oscillator have been given in figures 4.11 ,4.12, 4.13, 4.14.

Fitting a Damped Harmonic Oscillator

The harmonic oscillator and its damped variation have been widely used to study different systems across different areas. This is mainly due to its simplicity and has an exact solution (Berman and Cederbaum, 2018,Lima and Cohen, 1998). The damped version emulates a normal oscillator that starts to get damped after a few

oscillations. The general equation for the damped harmonic oscillator is as follows (Berman and Cederbaum, 2018):

$$m\frac{d^2x(t)}{dt^2} + b\frac{dx(t)}{dt} + kx(t) = F(t) \quad \text{where} \quad x^{(n)}(0) = x_0(n) \quad (n = 0, 1) \tag{4.7}$$

Equation 4.7 is representative of the second law of motion where $b\frac{dx(t)}{dt}$ is the velocity of the body that is neutralised by the friction $F_f = -b\frac{dx(t)}{dt}$. The stiffness is determined by Hooke's Law where $F_s = --kx(t)$. $\frac{d^2x(t)}{dt^2}$ is the rate at which the body accelerates and m is the mass. $F(t)$ is the driving force (Berman and Cederbaum, 2018, pp 744-745).

The equation can further be simplified in terms of angular frequency as it is an oscillatory motion. Assuming that the damping is exponential, solving equation 4.7 leads to the following solution (Berman and Cederbaum, 2018, p 751) :

$$x(t) = Ae^{-\beta t}\cos(\omega t - \phi) \tag{4.8}$$

where A is the amplitude at the initial position , β is the decay or damping parameter, ω is the angular frequency and ϕ is the phase angle in radians. For calculation purposes the phase has been set to zero and the amplitude has been set to 1 since the ACF starts at 1.

The oscillator function has been set to a non-linear regression model using least squares. The least squares method is commonly used technique to fit non-linear functions (Simpson and Montgomery, 1998). The main goal is to find the parameters that minimise the difference between the actual values and the predicted ones for which the objective function is given by (Barham and Drane, 1972, p 758):

$$Q(\theta) = \sum_{i=1}^{n}[y_i - f(x_i;\theta)]^2 \tag{4.9}$$

where $Q(\theta)$ is the cost/error for the optimal parameter vector θ. y is the vector of

the real values or dependent variable and x is the independent variable vector.

However, the least squares method can be more sensitive to outliers due to the squared error. A robust regression method has been used where the weights have been updated iteratively based on the weights in the preceding iteration. This process continues until convergence where the effect of outliers diminishes (Simpson and Montgomery, 1998). In order to this, the MATLAB's nlinfit function with the robust weighting option has been used. Moreover, the initial parameters have been set using the Random Sample Consensus (RANSAC) method which is an efficient method to interpret data with anomalies or large errors (Fischler and Bolles, 1981). Unlike other robust estimation methods like the M-estimate that use highly complex non-linear functions and have computational complexity, RANSAC is a fairly simple process . It is also a common tool for 'model fitting'(Choi, Kim, and Yu, 2009, p 1). The RANSAC algorithm has been implemented in the project in just few steps as given below:

- Initialise the range for the number of iterations.
- Randomly iterate from sample data with initial parameters to fit the model.
- Calculate the least absolute error (LAE) or the L1 norm between the predicted output and actual output for every iteration. Absolute error has been used since it is more robust to outliers than least squares. The formula for LAE is (Ding and Jiang, 2017):

$$E = \sum_{i=1}^{n} |y_i - f(x_i)| \tag{4.10}$$

  where E is the error and y_i is the actual value and $f(x)$ is the predicted value.
- Continue the process until the weights converge and the error is minimised to use as the optimal parameters.

Using the optimal weights from the RANSAC method along with with the robust settings, the model has been fitted to the ACF.

Finally, the performance of the model for fitting the ACF has been evaluated using MSE (Mean Squared Error). MSE is a suitable measure since the original values can be compared to the regression model predictions (Simpson and Montgomery, 1998). The formula for MSE is given by (Wang and Bovik, 2009, p 99):

$$MSE = \frac{1}{n}\sum_{i=1}^{n}(y_i - f(x)_i)^2 \tag{4.11}$$

It was observed that for an exponential function, the model had to be run multiple times to find a good fit for the model. Thus the exponential function has been represented in its fractional form. It is found that decay models with oscillating frequency and amplitude such as the damped harmonic oscillator can be represented by any other sustainable forms of $\omega(E)$ (Urbanowski, 2017). $\omega(E)$ is the spectral density that is the Fourier Transform of the ACF as given in (Wittke, 1964) and references within. Using the Bernoulli Inequality Principle the following can be derived (Y. Li and Yeh, 2013):

$$e^x \geq 1 + x$$

Substituting in the above, we get:

$$e^{-}x \leq \frac{1}{1+x} \tag{4.12}$$

Finally, replacing equation 4.12 in equation 4.8 we get the fractional form where $A = 1$ and $\phi = 0$ we get :

$$x(t) = A\frac{1}{1+\beta t}\cos(\omega t - \phi) \tag{4.13}$$

The angular frequency has been converted to regular frequency. Frequency f for

a periodic signal is defined as the inverse of time period which is given by (Eckhardt, Hippe, and Hosemann, 1989) where f is measure in $(Hertz)Hz$ and T is in $seconds(s)$:

$$f = \frac{1}{T}$$

Further, ω, the angular frequency is measured in $radian/s$ and can be converted to F in Hz by (Eckhardt, Hippe, and Hosemann, 1989) :

$$f = \frac{\omega}{2\pi} \tag{4.14}$$

In the model, ω has been calculated for every time-frame. Thus, to get the angular frequency per second, 4.14 has been multiplied by the frame rate (r) for each video which is given in $frames/sec$ as given below:

$$f = \frac{\omega r}{2\pi} \tag{4.15}$$

Validating the model

In-order to validate this method, the model has been fitted to sample data. Both the methods using the exponential form (equation 4.8 and the fractional form (equation 4.13). Both the methods as can be seen in the figures (refs) result similar results. Further, the plots also show that the damped harmonic oscillator manages to find a good fit for different damping/decay values such as the sine wave in figure 4.9 that has zero damping. Additionally, the model has been tested on real data. Figure 4.10 shows the ACF for sunspot time series which is a commonly used public dataset to evaluate models. The sunspot data contains the monthly mean sunspot numbers from the 1700s to current date. The time series used for the ACF has been taken from 1749 to 1893 (SILSO World Data Center, n.d.).

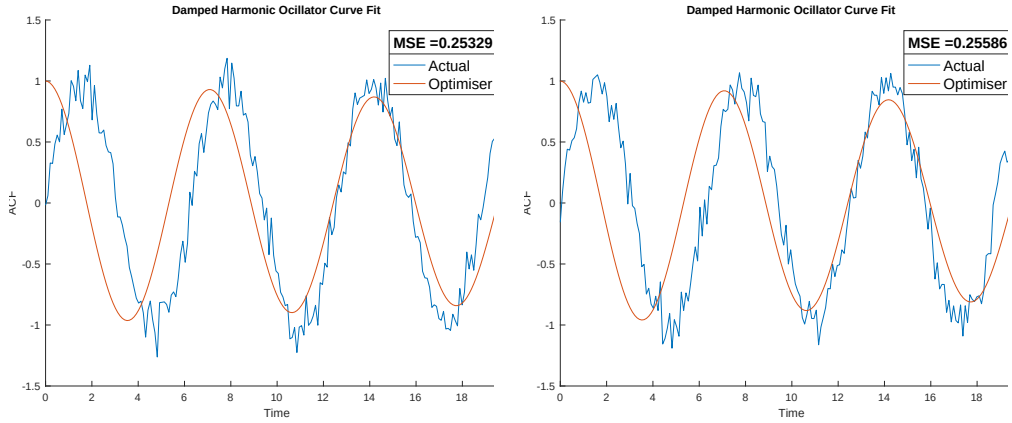

FIGURE 4.9: a) The plot on the left depicts the curve fit for a noisy sine wave over different time lags using the fractional form as given in eq. 4.13 b) The plot on the right depicts the curve fit for a noisy sine wave over different time lags using the exponential form as given in eq. 4.12

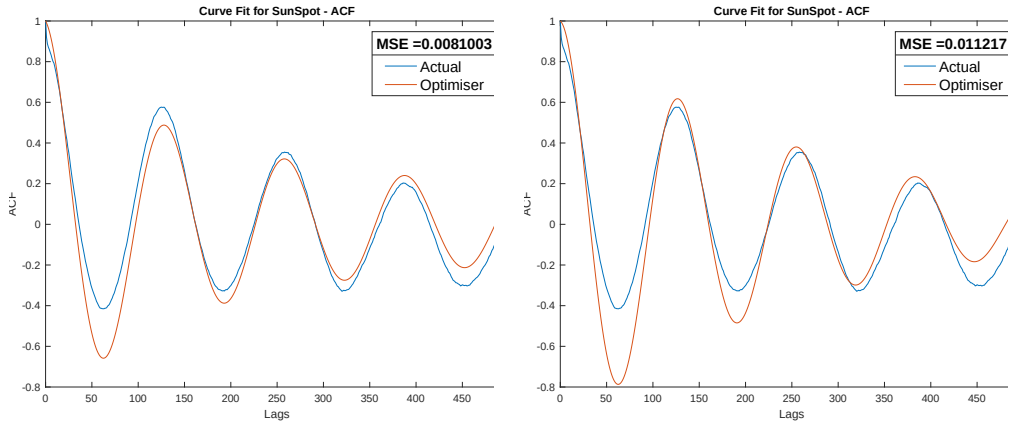

FIGURE 4.10: a) The plot on the left depicts the curve fit for the Sunspot Time series ACF wave using the fractional form as given in eq. 4.13 b) The plot on the right depicts the curve fit for Sunspot Time series ACF using the exponential form as given in eq. 4.12

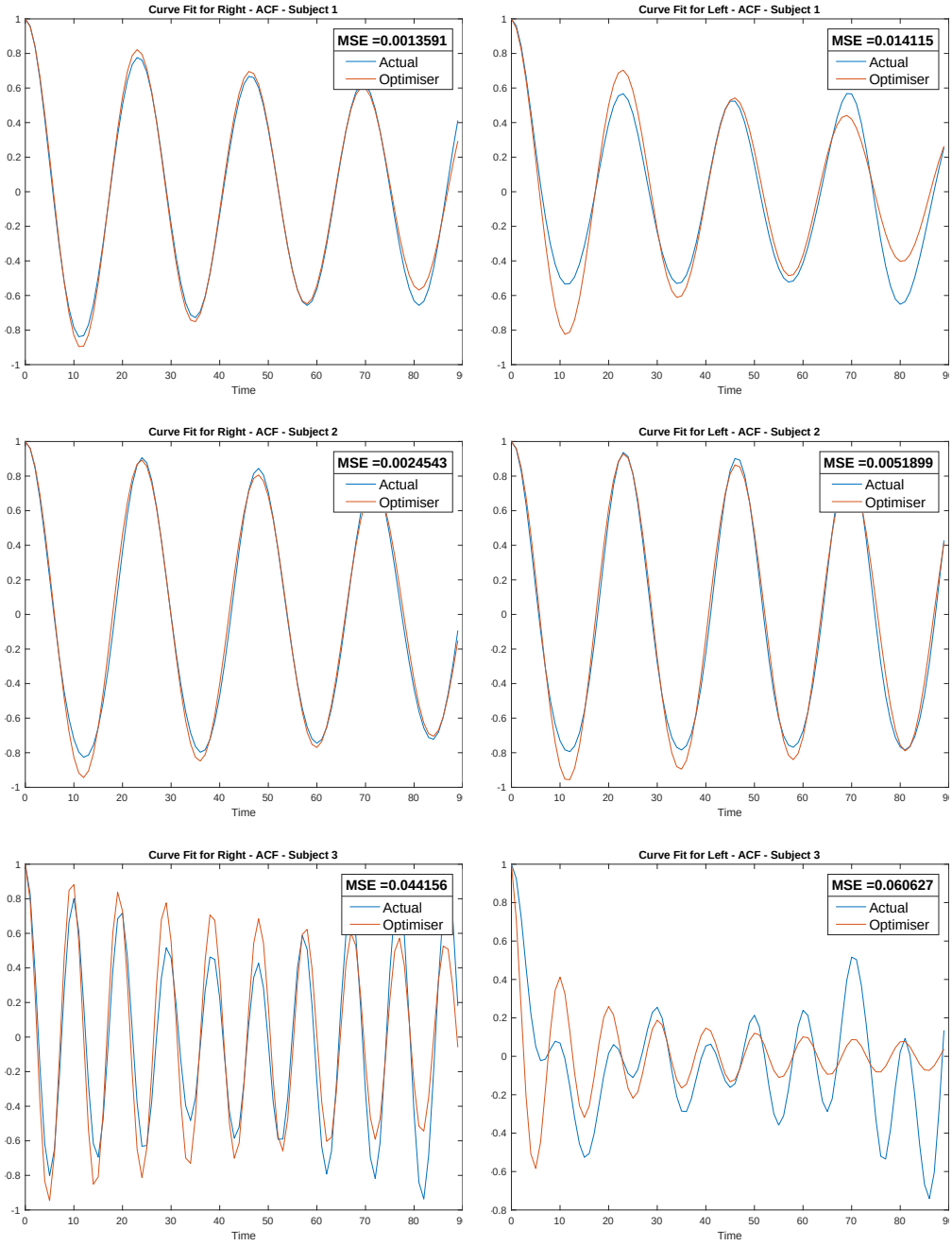

FIGURE 4.11: Model Fitting for ACF for the different subjects.

The damped model has been fit to the ACFs for the left and right hands for different subjects

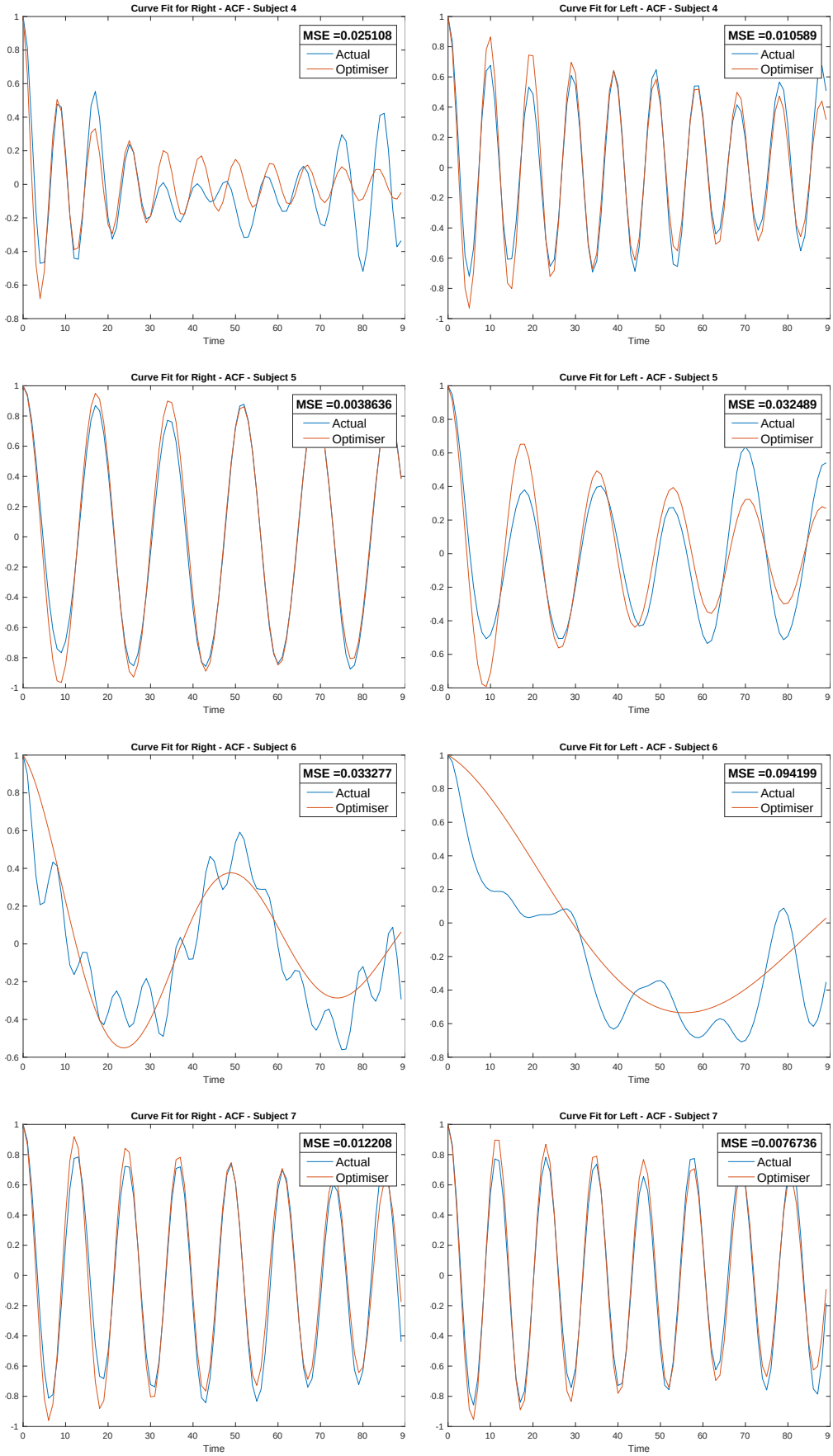

FIGURE 4.12: Model Fitting for ACF for the different subjects

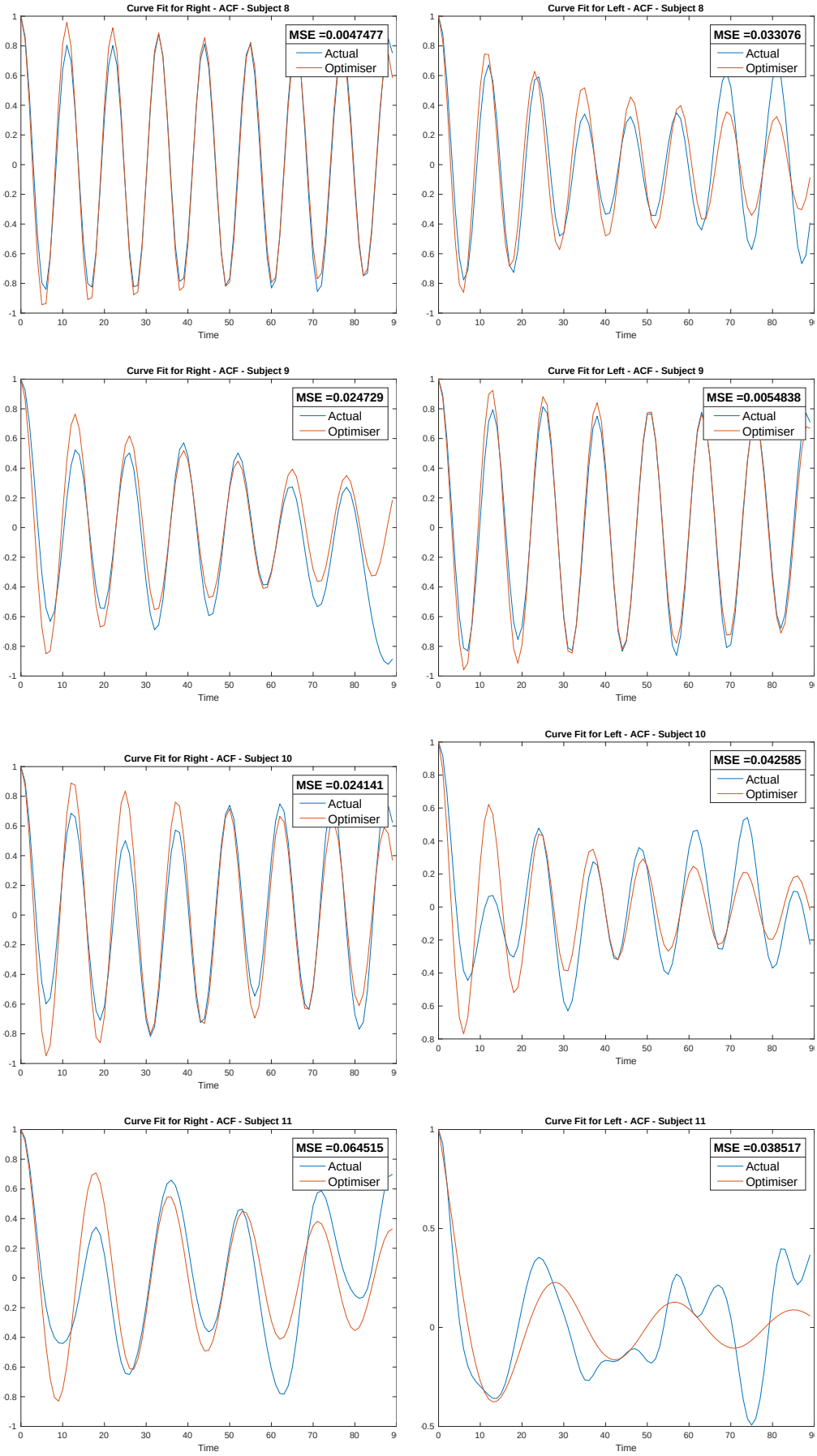

FIGURE 4.13: Model Fitting for ACF for the different subjects

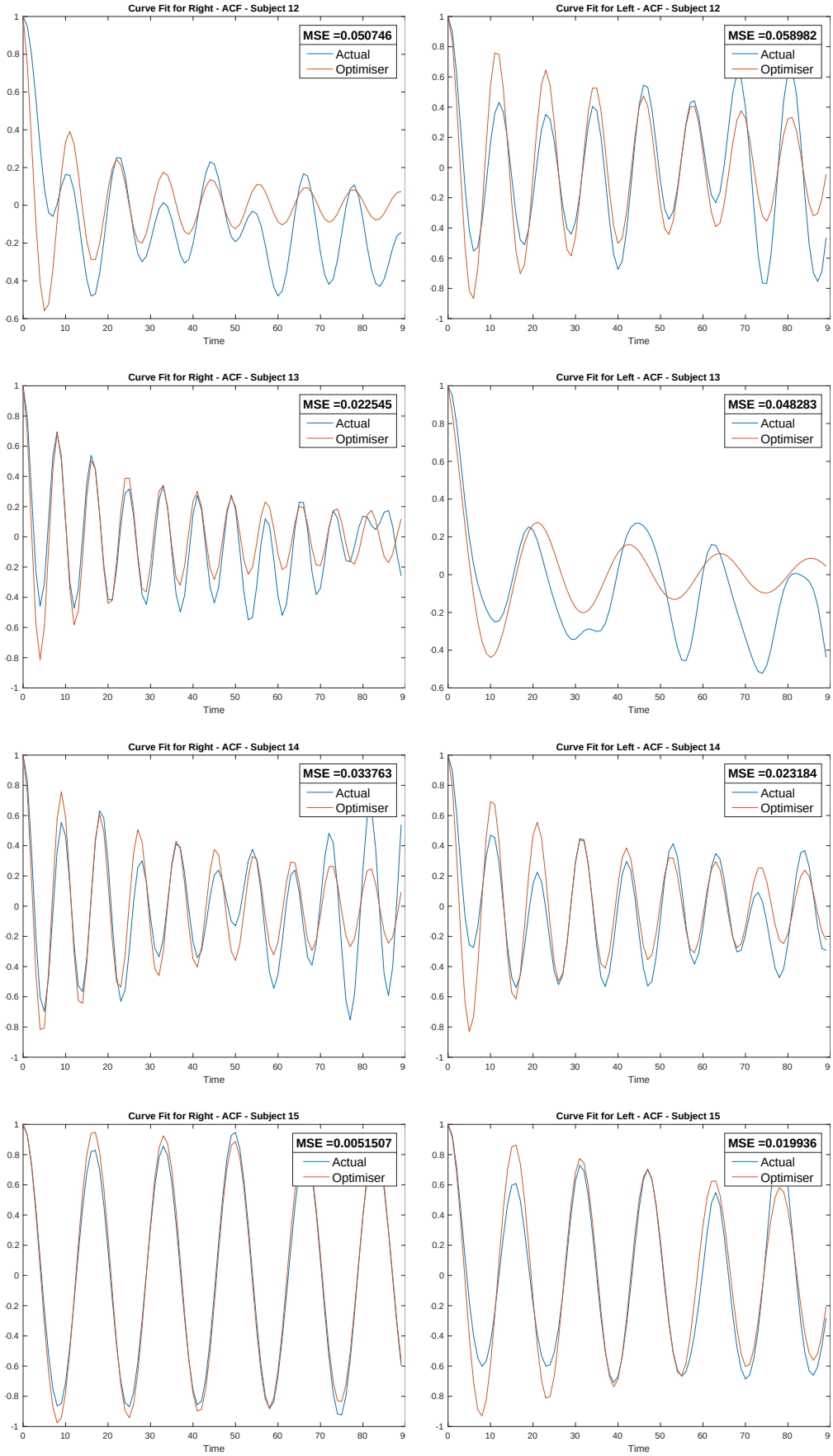

FIGURE 4.14: Model Fitting for ACF for the different subjects

The metrics tapping frequency and the decay in tapping amplitude that have been extracted using the damped harmonic oscillator have been listed in the results section.

RMS Amplitude

One limitation of the ACF is that it does not capture the original amplitude since it is mostly focused on the correlation between the signals and not the actual length (Nelson-Wong et al., 2009). Therefore, the Root Mean Square (RMS) level has been used to determine the tapping amplitude. This method computes the square root of average sum of squared values (Novotny and Sedlacek, 2008). It can be used to estimate significant changes in amplitude which in this case are the peaks (Saravanan, Gopalakrishnan, and Rao, 2015). If the signal is spaced in equally across the time, then the RMS formula is given by (IEEE Std 181, 2003, p 5) :

$$y_{rms} = \sqrt{\frac{1}{n}\sum_{i=1}^{n} y_i^2} \tag{4.16}$$

The RMS values for the left and right hand have been recorded in the results section.

4.3.5 Classification

The final step was to use the extracted features to classify the dominant hand and non-dominant hand. An SVM and a Naive Bayes classifier have been used to do this linear classification.

SVM

A support vector machine (SVM) is a widely used supervised learning algorithm for binary classification. Further it can also be extended to multi-class classification. An SVM has been chosen over other ML techniques such as decision trees

and neural networks is because of its simplicity and ability to give good accuracy on small datasets. SVM tends to generalise better for unseen data than neural networks where the objective is to minimise the training error (Mathur and Foody, 2008, p 241). Previous work in classification for PD have outlined the efficiency in using an SVM (Khan et al., 2014, Martinez-Manzanera et al., 2016). The main objective of an SVM is to fit a hyperplane that separates the classes optimally with a focus on the training points found at the corners of the distributions for the classes. These corner points are the support vectors. Hence, only the support vectors are requisite for determining the decision boundary (Mathur and Foody, 2008, p 241). The equation for a linear SVM is given by as stated in (Mathur and Foody, 2008, p 242):

$$\mathbf{y}_i(\mathbf{w} \cdot \mathbf{x}_i + \mathbf{b}) - 1 \geq 0 \tag{4.17}$$

where $(\mathbf{w} \cdot \mathbf{x}_i + \mathbf{b})$ is the hyperplane which in this case is linear where $(\mathbf{w} \cdot \mathbf{x}_i + \mathbf{b}) \geq +1)$ (when $y_i = +1$) and $(\mathbf{w} \cdot \mathbf{x}_i + \mathbf{b}) \geq -1)$ (when $y_i = -1$) which are the support vectors. $\mathbf{x}$ is the data point and $\mathbf{w}$ is perpendicular to the plane and $\mathbf{b}$ is the bias term.

From equation 4.17, the separation between the hyperplanes becomes $\frac{2}{|w|}$. Thus, the cost function subjected to constrained optimisation is to be minimised:

$$\min\{\frac{1}{2}||\mathbf{w}||^2\} \tag{4.18}$$

When the hyperplane is non-linear, slack parameters $\{\xi_i\}_{i=i}^{r}$ are added and the equation becomes :

$$\mathbf{y}_i(\mathbf{w} \cdot \mathbf{x}_i + \mathbf{b}) \geq 1 - \{\xi_i\}_{i=i}^{r} \tag{4.19}$$

When slack values ξ_i are very large, equation 4.19 is usually penalised by an additional term $C\sum_{i=1}^{r}\xi_i$ and the equation becomes :

$$\min[\frac{1}{2}||\mathbf{w}||^2 + C\sum_{i=1}^{r}\xi_i] \tag{4.20}$$

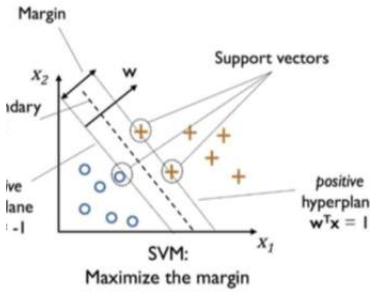

FIGURE 4.15: Linear separating Hyperplane with the support vectors as given in (Raschka and Mirjalili, 2017, p 138)

The linear SVM has been implemented in python using skikit-learn library (Pedregosa et al., 2011). Further, to improve the accuracy and reduce overfitting, the hyperparameter C for linear SVM has been tuned using a grid search algorithm. Grid Search is a basic 'exhaustive search' technique where a range of values are set for the hyperparameter. The program assesses the implementation for different combinations to get the most suitable value form the specified range (Pedregosa et al., 2011, p 312).

The accuracy for the model has been given in the results section.

Naive Bayes

The second model that has been used for classification is the Naive Bayes model. Naive Bayes (NB) has also been used for classifying neurological diseases such as in (Baby, Saji, and C. S. Kumar, 2017). An advantage of using Naive Bayes is that it does not require large amounts of training data like the SVM to find the optimal parameters to classify the data. Another difference is that in NB, the parameters

for probable hypothesis are not searched explicitly unlike other methods. On the other hand, the optimal values are found by calculating the frequency of different combinations of training samples (T.M. Mitchell, 1997, p 178).Under Naive Bayes, it is assumed that all variables are independent and as such, only the diagonal elements of the covariance matrix that contain the variance are needed for evaluation (D. Kumar et al., 2015, p 11). As the name suggests, Naive Bayes is based on the Bayes theorem where the the variables are conditionally independent. The conditional probability for independent events is the product of the prior probabilities as given below (T.M. Mitchell, 1997, p 177):

$$P(a_1, a_2, ...a_n) = \prod_i P(a_i|v_j) \tag{4.21}$$

Substituting equation4.21 in Bayes theorem , the function for Naive Bayes is (T.M. Mitchell, 1997, p 177):

$$v_{nb} = \text{argmax}_{v_j \in V} \prod_i P(a_i|v_j) \tag{4.22}$$

where v_{nb} is the prediction target.

4.3.6 Classifier Performance Evaluation

The performance of the classifiers is evaluated by comparing the accuracy on the test data. Further a confusion matrix can be used to compute other metrics such as Precision, Recall and F-Score. The confusion matrix depicts the classification errors between the predicted and actual class and gives true classification and false classification values (Gonzalez-Abril et al., 2017).

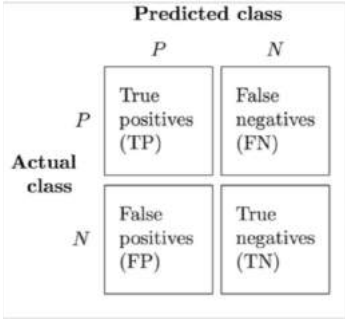

FIGURE 4.16: Confusion Matrix as given in (Raschka and Mirjalili, 2017, p 319)

On the basis of the confusion matrix, the recall determines the percentage of positive values that have been classified correctly and is given by (Gonzalez-Abril et al., 2017, p 662):

$$Recall = \frac{TP}{N_{positive}} \quad \text{where N is the number of actual positive values} \tag{4.23}$$

Precision on the other hand measures what proportion of all the values that have been classified as positive are actually true positive and is given by (Gonzalez-Abril et al., 2017, p 662):

$$Precision = \frac{TP}{TP + FP} \tag{4.24}$$

The F-score combines the precision and recall metrics and is given as below: (Gonzalez-Abril et al., 2017, p 662):

$$F - Score = \frac{Precision \cdot Recall}{\beta^2 Recall + Precision} \tag{4.25}$$

where usually $\beta = 1$ which is the tuning constant.

Another common measure to compare classifier performance are the ROC (Receiving Operating Characteristic) Curves. Although for imbalanced data such as the current data , ROC curves can be mis-representative of the actual performance (Saito

and Rehmsmeier, 2015). Thus, the accuracy, precision, recall and f-score metrics for both the classifiers have been given in the Results section.

Chapter 5

Results

The extracted features from the model fitting for decay and frequency as well as the RMS amplitude have been given in the tables **??**and **??** for left hand and right hand for all the videos. Essentially, the dominant hand would have a higher tapping frequency, a lower decay and a larger amplitude. On the other hand, the non-dominant hand would have a lower tapping frequency, a larger decay and a lower amplitude (Hubel et al., 2013).

TABLE 5.1: Extracted Features for Left Hand

ubject 1	Right	0.0722	0.0577	0.551	27.0602
ubject 1	Right	0.0183	0.2734	2.6108	26.5914
ubject 2	Left	0.0033	0.2711	2.5888	34.6764
ubject 3	Right	0.1422	0.6238	2.9784	64.4955
ubject 4	Left	0.0143	0.644	3.0749	33.3332
ubject 5	Right	0.029	0.3559	1.6993	34.2861
ubject 5	Right	0.0377	0.3692	1.7628	39.6299
ubject 6	Right	0.0152	0.0537	0.2564	30.3168
ubject 7	Right	0.0066	0.5455	2.6046	74.2296
ubject 8	Right	0.0257	0.5439	2.5969	103.8274
ubject 8	Right	0.0123	0.5435	2.595	104.9978
ubject 9	Right	0.0049	0.4973	2.3744	46.1626
ubject 10	Right	0.0495	0.5131	2.2049	13.5044
ubject 11	Right	0.1203	0.221	1.0552	20.9428
ubject 12	Right	0.0241	0.5456	2.1709	25.2591
ubject 12	Left	0.0245	0.5537	2.2031	25.8323
ubject 12	Left	0.0097	0.4951	1.9699	22.9669
ubject 13	Left	0.1231	0.2938	1.4028	33.6896
ubject 14	Right	0.038	0.5982	2.8562	104.6508
ubject 15	Right	0.0091	0.4016	1.9175	62.9462

TABLE 5.2: Extracted Features for Right Hand

ubject 1	Right	0.0094	0.2711	2.5888	32.4993
ubject 2	Left	0.005	0.2623	2.5048	39.7976
ubject 3	Right	0.0096	0.6542	3.1236	34.9224
ubject 4	Left	0.114	0.7525	3.5929	22.9964
ubject 5	Right	0.0029	0.365	1.7427	31.0972
ubject 5	Right	0.0058	0.3822	1.8249	25.4194
ubject 6	Right	0.0335	0.1264	0.6035	15.2324
ubject 7	Right	0.0068	0.5151	2.4594	52.8092
ubject 8	Right	0.0038	0.5723	2.7325	113.6022
ubject 8	Right	0.0428	0.5791	2.765	99.1257
ubject 9	Right	0.0237	0.4835	2.3085	42.6659
ubject 10	Right	0.0078	0.5042	2.1666	16.4116
ubject 11	Right	0.0227	0.3529	1.685	18.5434
ubject 12	Right	0.1409	0.566	2.252	22.4271
ubject 12	Left	0.0016	0.5761	2.2922	21.2717
ubject 12	Left	0.0058	0.5366	2.1351	19.8236
ubject 13	Left	0.0565	0.7679	3.6665	69.0693
ubject 14	Right	0.0355	0.6928	3.3079	63.4413
ubject 15	Right	0.0024	0.3792	1.8105	51.5503

Also the correlation between the dominant and non-hand for all the subjects has been plotted below:

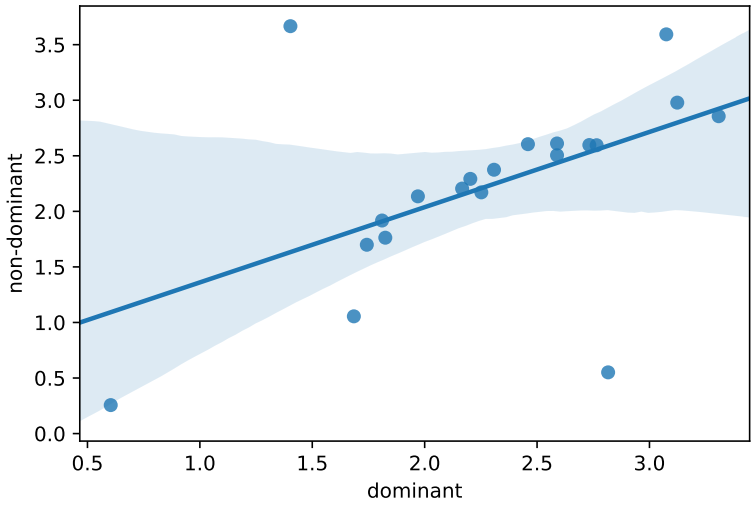

FIGURE 5.1: Relationship between Dominant and Non-Dominant Hand

As can be seen in 5.1, the dominant and non-dominant hand have a positive correlation with a few outliers.

TABLE 5.3: Classifier Results

Classifier	**Accuracy**	**Precision**	**Recall**	**F-Score**
SVM	80 %	100 %	80 %	88.9%
Naive Bayes	75 %	100 %	75 %	85.7%

Further the confusion matrix has also been plotted below :

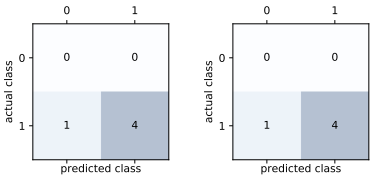

FIGURE 5.2: The confusion matrix for a) SVM b) Naive Bayes, where 0 denotes the left-handed class and 1 denotes the right-handed class. Further, the left-side has been assigned as the negative class and right as the positive class. It can be seen

Chapter 6

Discussion

6.0.1 Key Findings

Despite numerous research being done in biomarker detection for Parkinson's Disease, a simple, economical and sensitive biomarker is still yet to be made available. It is evident that despite extensive research, the UPDRS scores rating by the clinicians is still the most widely used assessment for PD. This is supported by prior research done in this area as highlighted in the earlier sections. In this project, we propose a cost-efficient and simple method to track the motor symptoms of PD. Although, this is not a groundbreaking innovation for biomarker detection, it definitely bridges the gap between the discrepancies that are prevalent whilst monitoring the disease such as the inter and intra-rater variability. As such, the calculated metrics would be more reliable due to the accuracy and exactness of the values. This can assist the clinicians in making better judgment whilst rating the subjects. Further, the cost of clinical trials would be significantly reduced if the errors and distortions in data have been minimised.

It was found that, video-related biomarkers are not being used in clinical practice on a large scale. However, research using computer vision and signal processing methods to analyse motor symptoms has been implemented. Although, majority of the proposed methods are not scalable due to system complexities and difficulty

in using the devices. Further most of these methods have also used wearable sensors to capture reliable data. As previously emphasized, wearable sensors might not be convenient for long-term patient monitoring due to the obvious reasons such as inconvenience to the patients. Additionally, the video camera system has been set up in specific conditions using complex technology. Whereas, in this case videos have been recorded using a mobile phone camera and have been put through pose estimation using OpenPose. By setting up an analytics system that integrates OpenPose, the captured videos can be easily put through pose estimation and the relevant metrics can be extracted.

Recent research has been done using OpenPose to analyse gait (Deligianni et al., 2018. Also, CPM (precursor to OpenPose) has been used to identify PD patients from drug induced dyskinesia patients M. Li et al., 2017). However, these methods use 3D reconstruction and spectral analysis techniques to extract the features. These methods are more complex. In the case of spectral analysis, the signal has to be of a reasonable long length. Whereas in this project a simple and yet efficient method has been proposed to extract the features. The ACF of the series has been fitted to a damped harmonic oscillator model to extract the relevant features for which the results are given in tables 5.1 and 5.2. As can be seen in the results, it is shown that for the right and left hand cases, there is not much variation for both hands. In some cases, for some subjects the non-dominant hand has a higher parameter values than the dominant hand. This can be due to the short duration of the clip. As only 4 seconds of tapping rate have been included. This was because of missing data that had to be discarded. In prior research by (Hubel et al., 2013), a 30-second time series has been used to see the variation in the tapping frequency, amplitude and other parameters.

Finally, the extracted features have been classified using binary classifiers such as SVM and Naive Bayes for which the results are given in 5.3. Due to the nature of the dataset that was highly imbalanced and had a small sample size. It had total of

21 videos amongst which 15 right-handed subject videos and only 6 videos with a dominant left hand, the accuracy results might be biased. This is the reason why the precision and recall scores and the confusion matrices might not be giving a true picture of the data. Despite the bias, the classifier does give a good accuracy considering the limitations of the dataset.

6.0.2 Limitations

The main limitation for the project has been the data. The reason why gait analysis could not be proceeded was due to poor video capturing. This is also the case for finger-tapping data for the patients. Thus, data has been simulated using healthy subjects for handedness which has been used as a test case. In most cases the data has been captured well, although due to the short duration as well as missing frames from the pose estimation, major portions of the signal have been discarded. If the time series was longer, the differences in results for the two classes would have been more prominent. However, the method can be applicable to real patients with the minimal changes in the process. This is because changes in motor patterns for finger-tapping and gait are more prominent in PD patients than in healthy subjects. This is the reason why not many differences have been observed for handedness over a short period of 4 seconds. Moreover, small dataset with a fewer samples for left-handed people had an impact on the results. Had there been more time, the data collection would have been done in a more organised fashion with an equal proportion in the data classes.

6.0.3 Future Work

There is scope for future work for the project. The methodology can be applied to extract key features from real PD patients. The most important aspect is in the way the data has been captured. If the videos have been taken in the current manner with

the entire person in frame with no disturbances, the techniques used in this project might produce reliable measures that can help find efficient neuromotor biomarkers for PD. Also, it can be collated with the UPDRS scores to predict the score from the frequency and decay parameters. Further, this research can also be extended to classifying different forms of parkinsonism on the basis of the motor patterns. This can be extremely important during the early stages since most patients are given the drugs used for PD for other conditions. Consequently can lead to drug induced side-effects such as dyskinesia in patients (Schlossmacher and Mollenhauer, 2010). Prior research has been done in classifying different forms of parkinsonism using public datasets that extracted features from sensors (Das, Saji, and C. S. Kumar, 2017).This research differs from previous research because it is very simple to capture accurate data from videos provided the basic guidelines are followed to get good data. By extracting features from video, several aspects of diagnosing PD can be made easier to interpret. This in turn can significantly reduce the cost of clinical trials and improve the treatment and care for PD patients. The techniques are not only restricted to PD but can be applied to diagnose other neurological and non-neurological conditions with motor symptoms. Lastly, the hand dominance criteria can also be tested in PD patients to explore the relation between the onset of symptoms on the dominant side.

6.0.4 Summary

In this study, a novel way to extract features for motor symptoms for Parkinson's Disease using a damped harmonic oscillator has been presented.The method is easy to compute and does not require the signal to be long or stationary. By implementing pose estimation on video data and by following the approach presented in this project, relevant neuromotor biomarkers for PD can be extracted.

Chapter 7

Conclusion

In conclusion, a thorough analysis has been carried out for extracting motor biomarkers for Parkinson's Disease. A novel method using a damped harmonic oscillator has been proposed to extract the relevant features. This was followed by classifying the two groups based on their handedness. The handedness criteria has been used as a test case. By using the approach detailed in the project, accurate metrics can be extracted that can help in better diagnosis and monitoring of Parkinson's Disease patients.

Appendix A

Additional Plots and Tables

A.0.1 Normalised Time Series Plots

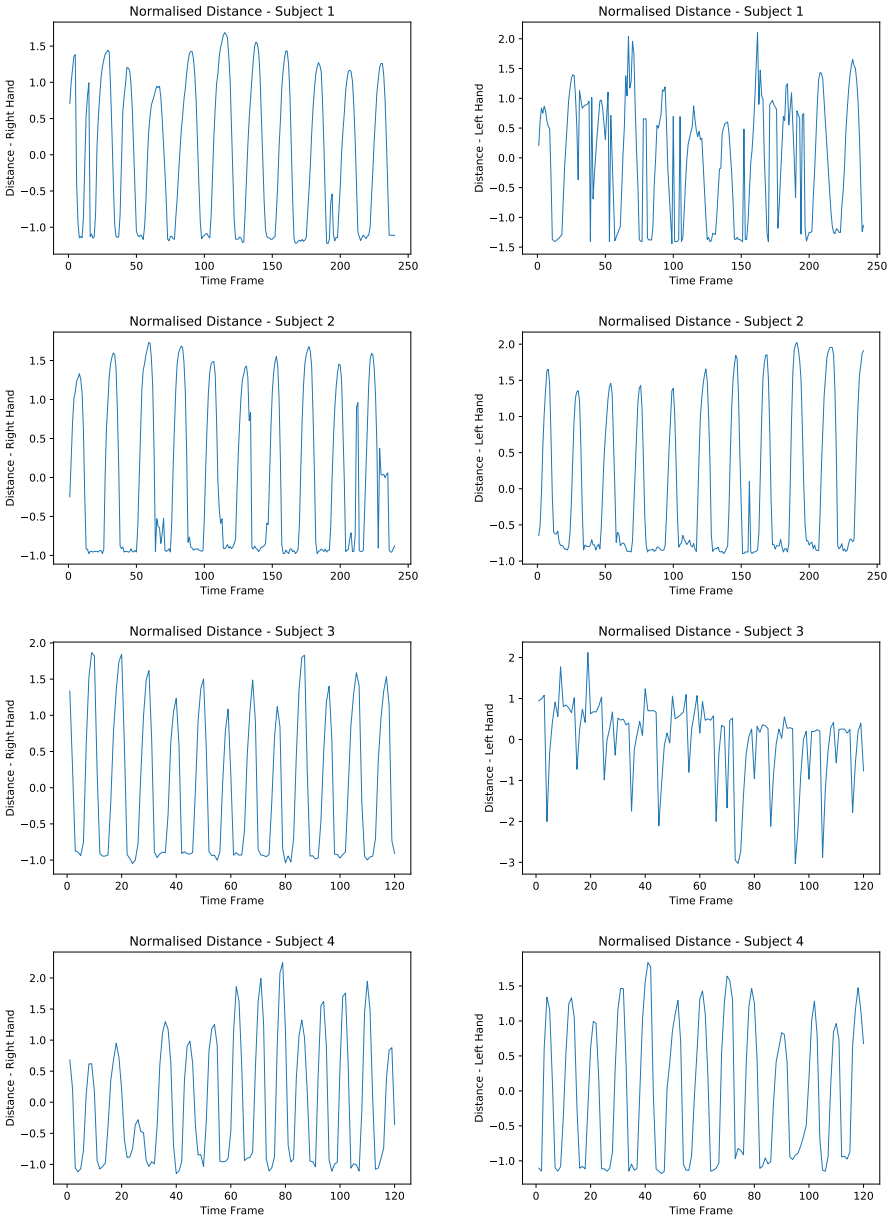

FIGURE A.1: Normalised Time Series for Right and Left Hand for all the subjects

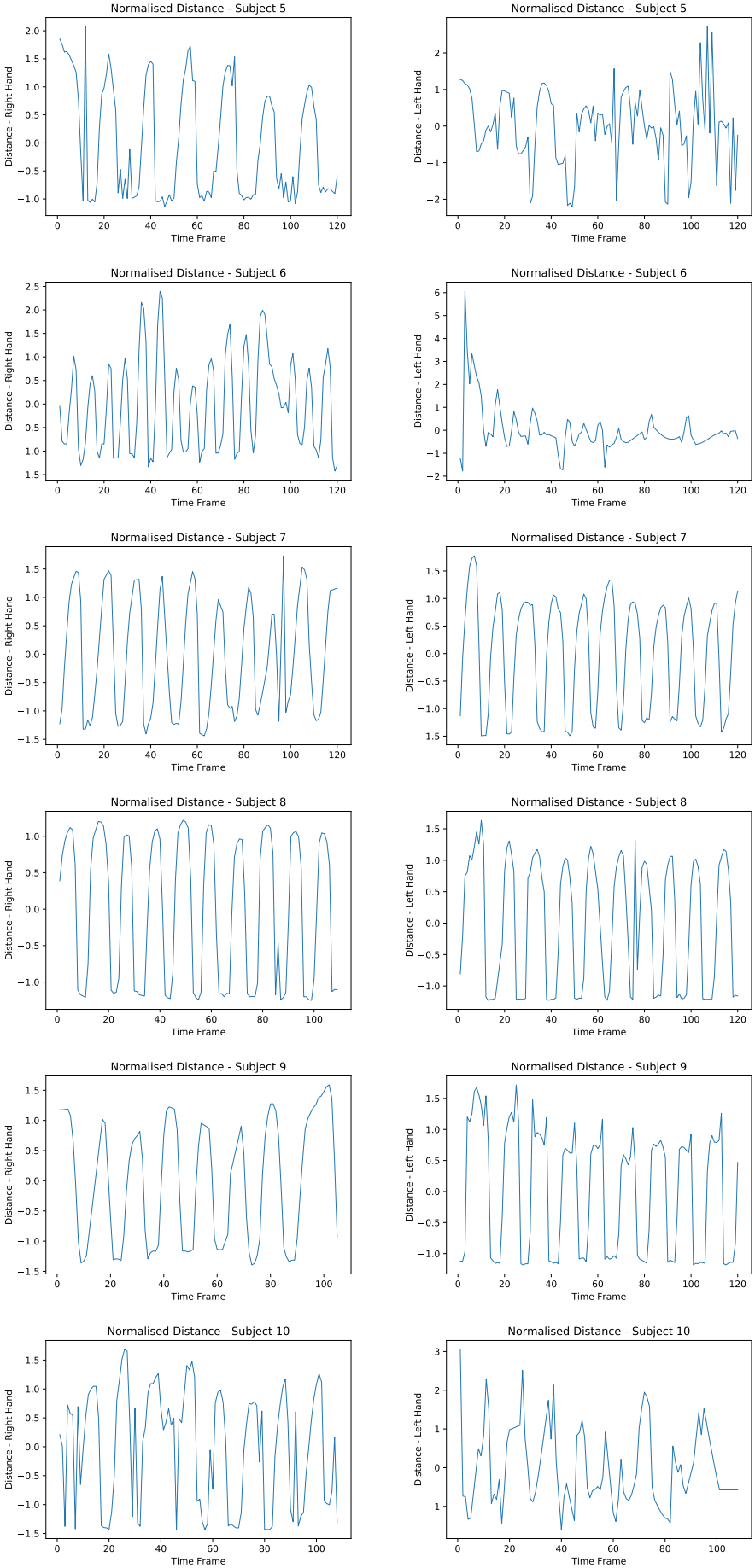

FIGURE A.2: Normalised Time Series for Right and Left Hand for all the subjects

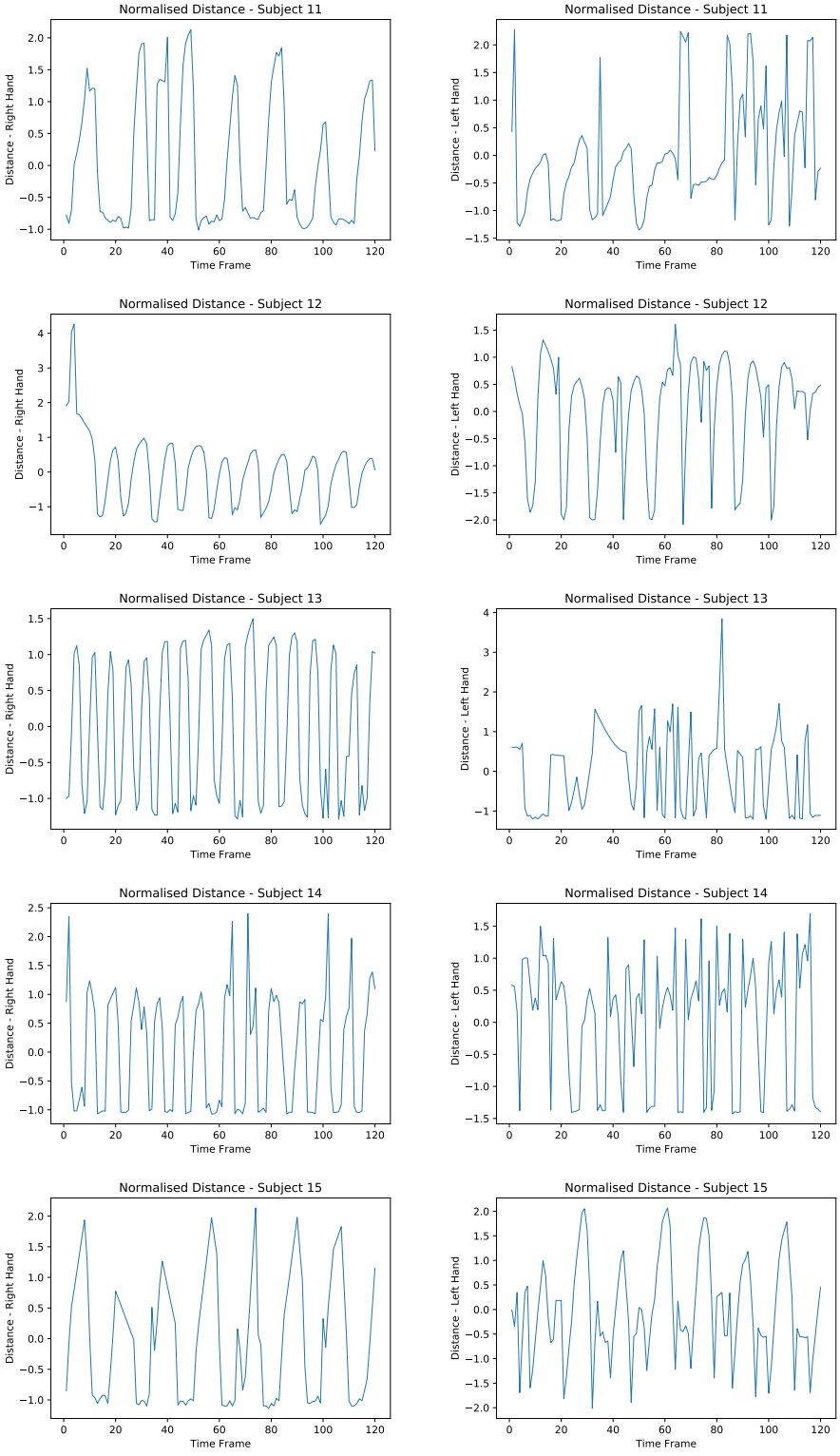

FIGURE A.3: Time Series for Right and Left Hand for all the subjects

A.0.2 ACF for all subjects

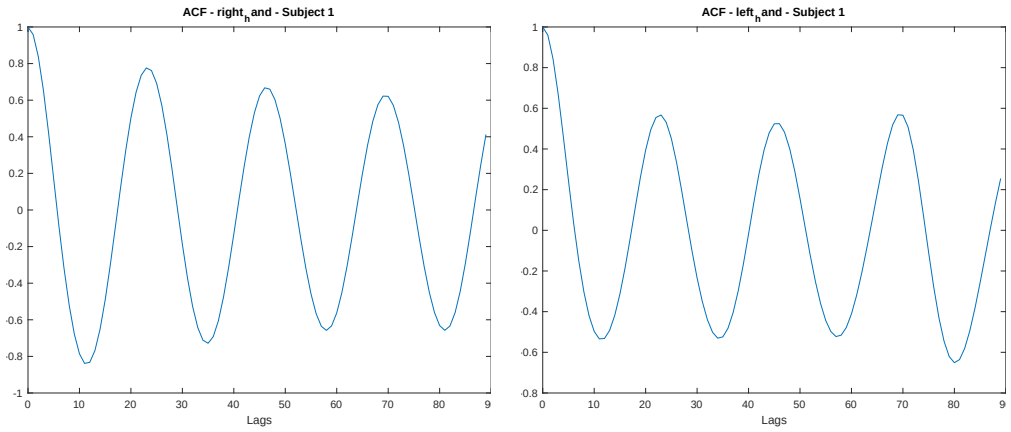

FIGURE A.4: ACF for the different subjects

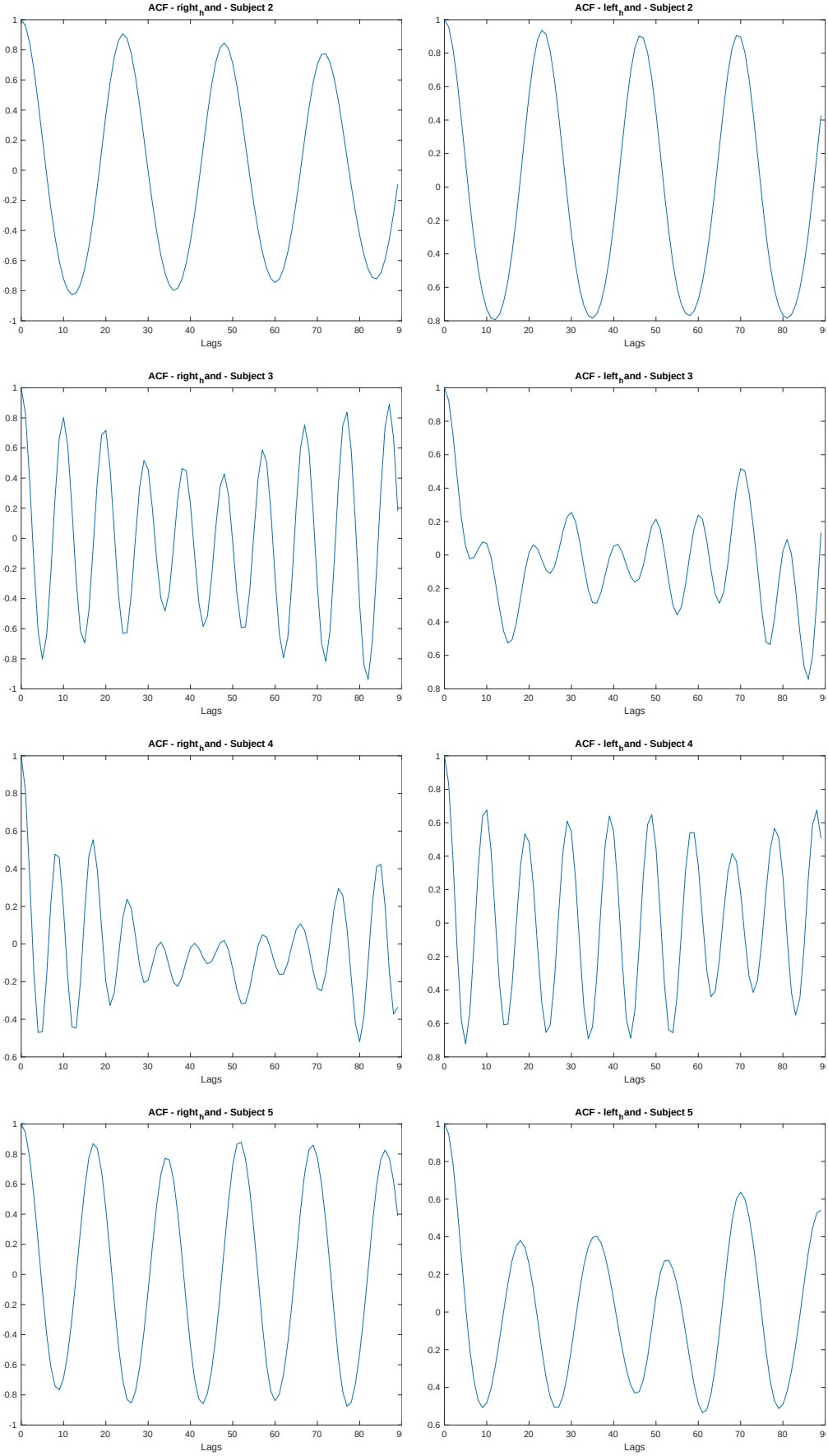

FIGURE A.5: ACF for the different subjects

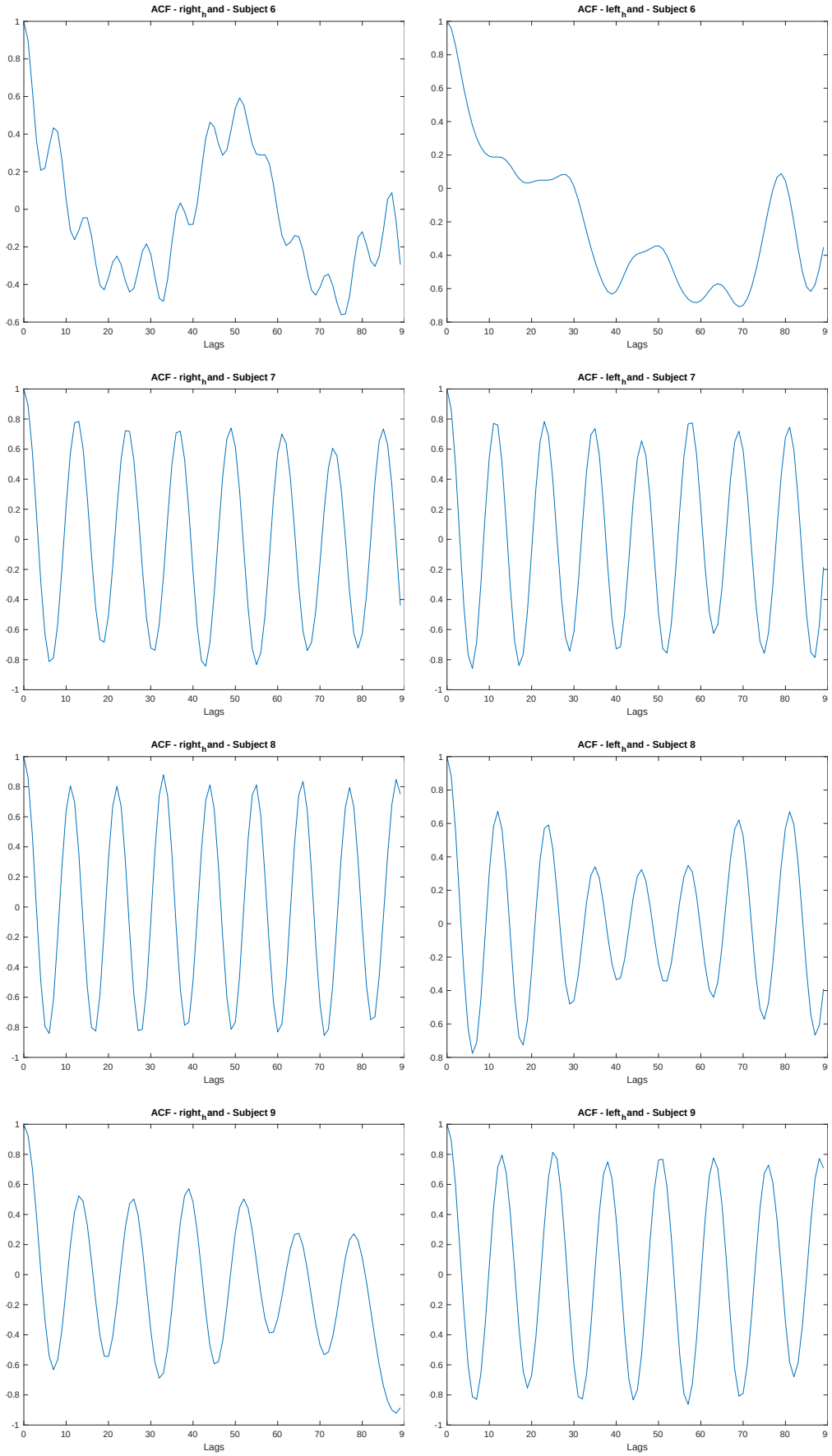

FIGURE A.6: ACF for the different subjects

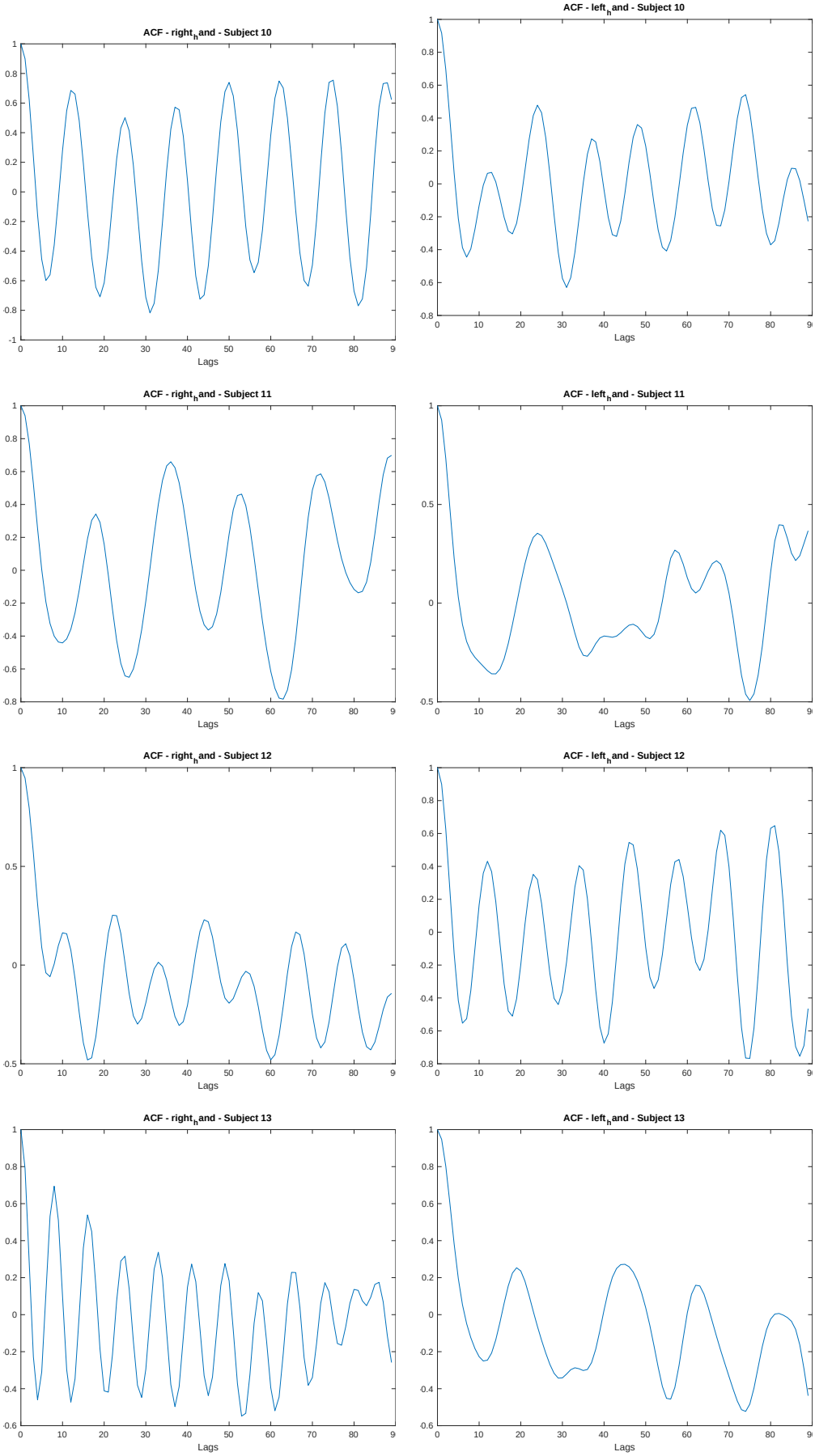

FIGURE A.7: ACF for the different subjects

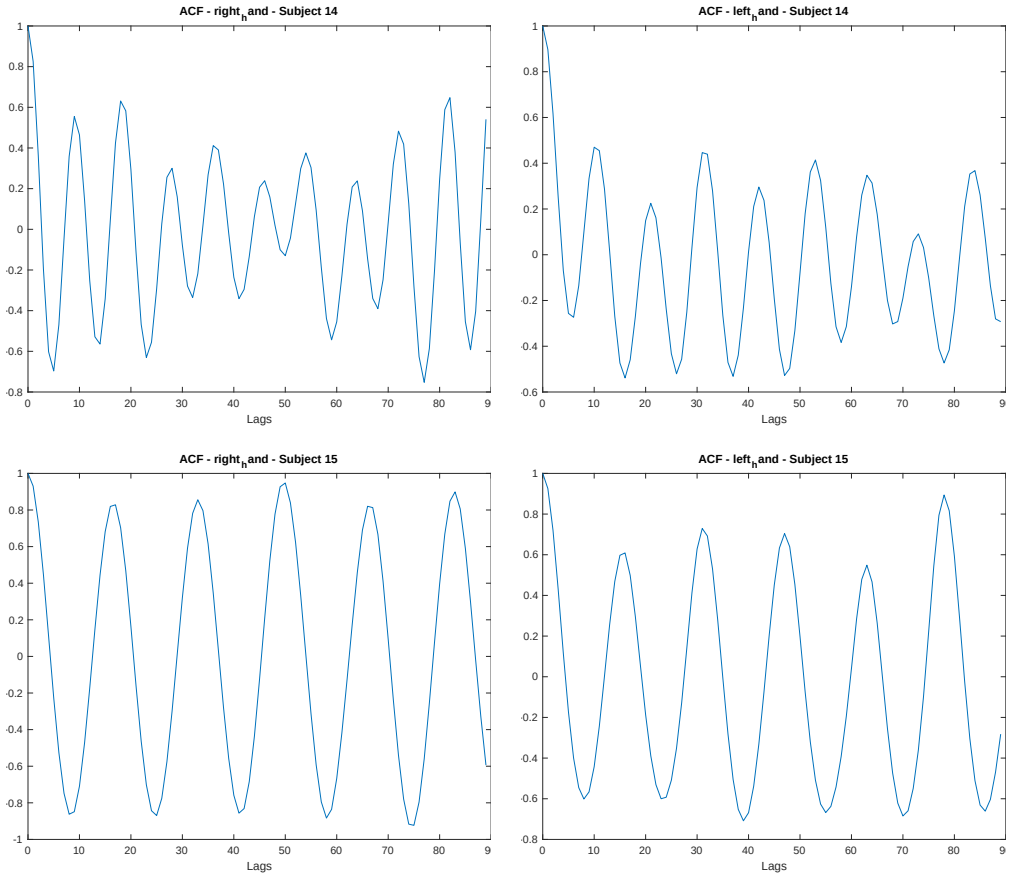

FIGURE A.8: ACF for the different subjects

Bibliography

Aoki, T., Rivlis, G., and Schieber, M.H. (2016). "Handedness and index finger movements performed on a small touchscreen". In: *Journal of Neurophysiology* 115.2. PMID: 26683065, pp. 858–867. DOI: 10.1152/jn.00256.2015. eprint: https://doi.org/10.1152/jn.00256.2015. URL: https://doi.org/10.1152/jn.00256.2015.

Artusi, C.A. et al. (2018). "Integration of technology-based outcome measures in clinical trials of Parkinson and other neurodegenerative diseases". In: *Parkinsonism & Related Disorders* 46. Proceedings of XXII World Congress of the International Association of Parkinsonism and Related Disorders, Ho Chi Minh City, Vietnam, 12-15 November 2017, S53–S56. ISSN: 1353-8020. DOI: https://doi.org/10.1016/j.parkreldis.2017.07.022. URL: http://www.sciencedirect.com/science/article/pii/S1353802017302699.

Baby, M. S., Saji, A. J., and Kumar, C. S. (2017). "Parkinsons disease classification using wavelet transform based feature extraction of gait data". In: *2017 International Conference on Circuit ,Power and Computing Technologies (ICCPCT)*, pp. 1–6.

Barham, R. H. and Drane, W. (1972). "An Algorithm for Least Squares Estimation of Nonlinear Parameters When Some of the Parameters Are Linear". In: *Technometrics* 14.3, pp. 757–766. ISSN: 00401706. URL: http://www.jstor.org/stable/1267303.

Barrett, M. J. et al. (2011). "Handedness and motor symptom asymmetry in Parkinson's disease". In: *Journal of Neurology, Neurosurgery, and Psychiatry* 82.10, pp. 1122–1124. DOI: 10.1136/jnnp.2010.209783. URL: http://doi.org/10.1136/jnnp.2010.209783.

Berardelli, A. et al. (2001). "Pathophysiology of bradykinesia in Parkinson's disease". In: *Brain* 124.11, pp. 2131–2146. DOI: 10.1093/brain/124.11.2131. eprint: /oup/backfile/content_public/journal/brain/124/11/10.1093/brain/124.11.2131/2/1242131.pdf. URL: http://dx.doi.org/10.1093/brain/124.11.2131.

Berman, M. and Cederbaum, L.S. (2018). "Fractional driven-damped oscillator and its general closed form exact solution". In: *Physica A: Statistical Mechanics and its Applications* 505, pp. 744–762. ISSN: 0378-4371. DOI: https://doi.org/10.1016/j.physa.2018.03.044. URL: http://www.sciencedirect.com/science/article/pii/S0378437118303649.

Bloem, B.R. (1992). "Postural instability in Parkinson's disease". In: *Clinical Neurology and Neurosurgery* 94. Neurodegeneration and Neuroprotection Postgraduate Boerhaave Course, pp. 41–45. ISSN: 0303-8467. DOI: https://doi.org/10.1016/0303-8467(92)90018-X. URL: http://www.sciencedirect.com/science/article/pii/030384679290018X.

Cao, Zhe et al. (2017). "Realtime Multi-Person 2D Pose Estimation using Part Affinity Fields". In: *CVPR*.

Cheadle, Chris et al. (2003). "Analysis of Microarray Data Using Z Score Transformation". In: *The Journal of Molecular Diagnostics* 5.2, pp. 73–81. ISSN: 1525-1578. DOI: https://doi.org/10.1016/S1525-1578(10)60455-2. URL: http://www.sciencedirect.com/science/article/pii/S1525157810604552.

Chen, Y.Y. et al. (2012). "A vision-based regression model to evaluate Parkinsonian gait from monocular image sequences". In: *Expert Systems with Applications* 39.1, pp. 520–526. ISSN: 0957-4174. DOI: https://doi.org/10.1016/j.eswa.2011.07.042. URL: http://www.sciencedirect.com/science/article/pii/S0957417411010049.

Cho, C.W. et al. (2009). "A vision-based analysis system for gait recognition in patients with Parkinson's disease". In: *Expert Systems with Applications* 36.3, Part 2, pp. 7033–7039. ISSN: 0957-4174. DOI: https://doi.org/10.1016/j.eswa.

2008.08.076. URL: http://www.sciencedirect.com/science/article/pii/S0957417408006003.

Choi, Sunglok, Kim, Taemin, and Yu, Wonpil (2009). "Performance Evaluation of RANSAC Family". In: *BMVC*.

ClinicalTrials.gov (2018). *Glossary of Common Site Ter*. URL: https://clinicaltrials.gov/ct2/about-studies/glossary (visited on 08/21/2018).

Das, K. Devi, Saji, A. J., and Kumar, C. S. (2017). "Frequency analysis of gait signals for detection of neurodegenerative diseases". In: *2017 International Conference on Circuit ,Power and Computing Technologies (ICCPCT)*, pp. 1–6. DOI: 10.1109/ICCPCT.2017.8074273.

Deligianni, F. et al. (2018). "A fusion framework to estimate plantar ground force distributions and ankle dynamics". In: *Information Fusion* 41, pp. 255–263. ISSN: 1566-2535. DOI: https://doi.org/10.1016/j.inffus.2017.09.008. URL: http://www.sciencedirect.com/science/article/pii/S1566253517302105.

Ding, C. and Jiang, B. (2017). "L1-norm Error Function Robustness and Outlier Regularization". In: *CoRR* abs/1705.09954. arXiv: 1705.09954. URL: http://arxiv.org/abs/1705.09954.

Djaldetti, R., Ziv, I., and Melamed, E. (2006). "The mystery of motor asymmetry in Parkinson's disease". In: *The Lancet Neurology* 5.9, pp. 796–802. ISSN: 1474-4422. DOI: 10.1016/S1474-4422(06)70549-X. URL: https://doi.org/10.1016/S1474-4422(06)70549-X.

Ebersbach, G. et al. (2006). "Scales in Parkinson's disease". In: *Journal of Neurology* 253.4, pp. iv32–iv35. ISSN: 1432-1459. DOI: 10.1007/s00415-006-4008-0. URL: https://doi.org/10.1007/s00415-006-4008-0.

Eckhardt, V., Hippe, P., and Hosemann, G. (1989). "Dynamic measuring of frequency and frequency oscillations in multiphase power systems". In: *IEEE Transactions on Power Delivery* 4.1, pp. 95–102. ISSN: 0885-8977. DOI: 10.1109/61.19193.

Espay, A. J. et al. (2016). "Technology in Parkinson disease: Challenges and Opportunities". In: *Movement disorders : official journal of the Movement Disorder Society*

31.9, pp. 1272–1282. DOI: 10.1002/mds.26642. URL: http://dx.doi.org/10.1002/mds.26642.

Fahn, S. (2018). "The 200-year journey of Parkinson disease: Reflecting on the past and looking towards the future". In: *Parkinsonism & Related Disorders* 46.S1, S1–S5. DOI: 10.1016/j.parkreldis.2017.07.020. URL: https://doi.org/10.1016/j.parkreldis.2017.07.020.

Fischler, M.A. and Bolles, R.C. (1981). "Random Sample Consensus: A Paradigm for Model Fitting with Applications to Image Analysis and Automated Cartography". In: *Commun. ACM* 24.6, pp. 381–395. ISSN: 0001-0782. DOI: 10.1145/358669.358692. URL: http://doi.acm.org/10.1145/358669.358692.

Flores, J. H. F., Engel, P. M., and Pinto, R. C. (2012). "Autocorrelation and partial autocorrelation functions to improve neural networks models on univariate time series forecasting". In: *The 2012 International Joint Conference on Neural Networks (IJCNN)*, pp. 1–8. DOI: 10.1109/IJCNN.2012.6252470.

Gao, J. et al. (2018). "Computer Vision in Healthcare Applications". In: *Journal of Healthcare Engineering*. 5157020. DOI: 10.1155/2018/5157020. URL: http://doi.org/10.1155/2018/5157020.

Goetz, C. (2011). "The History of Parkinson's Disease: Early Clinical Descriptions and Neurological Therapies". In: *Cold Spring Harbor Perspectives in Medicine:* 1.1. a008862, pp. 1–15. DOI: 10.1101/cshperspect.a008862. URL: https://doi.org/10.2217/bmm.10.93.

Goetz, C. et al. (2008). "Movement Disorder Society-sponsored revision of the Unified Parkinson's Disease Rating Scale (MDS-UPDRS): Scale presentation and clinimetric testing results". In: *Movement Disorders* 23.15, pp. 2129–2170. DOI: 10.1002/mds.22340. URL: https://onlinelibrary.wiley.com/doi/abs/10.1002/mds.22340.

Gonzalez-Abril, L. et al. (2017). "Handling binary classification problems with a priority class by using Support Vector Machines". In: *Applied Soft Computing* 61,

pp. 661–669. ISSN: 1568-4946. DOI: https://doi.org/10.1016/j.asoc.2017.08.023. URL: http://www.sciencedirect.com/science/article/pii/S1568494617305057.

Greche, L. et al. (2017). "Comparison between Euclidean and Manhattan distance measure for facial expressions classification". In: *2017 International Conference on Wireless Technologies, Embedded and Intelligent Systems (WITS)*, pp. 1–4. DOI: 10.1109/WITS.2017.7934618.

Gu, X. et al. (2018). "Markerless gait analysis based on a single RGB camera". In: *2018 IEEE 15th International Conference on Wearable and Implantable Body Sensor Networks (BSN)*, pp. 42–45. DOI: 10.1109/BSN.2018.8329654.

Hubel, K.A. et al. (2013). "Computerized Measures of Finger Tapping: Effects of Hand Dominance, Age, and Sex". In: *Perceptual and Motor Skills* 116.3. PMID: 24175464, pp. 929–952. DOI: 10.2466/25.29.PMS.116.3.929-952. eprint: https://doi.org/10.2466/25.29.PMS.116.3.929-952. URL: https://doi.org/10.2466/25.29.PMS.116.3.929-952.

IEEE Std 181 (2003). "IEEE Standard on Transitions, Pulses, and Related Waveforms". In: pp. 1–54. DOI: 10.1109/IEEESTD.2003.94394.

Jankovic, J. (2008). "Parkinson's disease: clinical features and diagnosis". In: *Journal of Neurology, Neurosurgery & Psychiatry* 79.4, pp. 368–376. ISSN: 0022-3050. DOI: 10.1136/jnnp.2007.131045. URL: https://jnnp.bmj.com/content/79/4/368.

Jankovic, J. and Stacy, M. (2007). "Medical Management of Levodopa-Associated Motor Complications in Patients with Parkinson's Disease". In: *CNS Drugs* 21.8, pp. 677–692. ISSN: 1179-1934. DOI: 10.2165/00023210-200721080-00005. URL: https://doi.org/10.2165/00023210-200721080-00005.

Jordan, M. and Mitchell, T. (2015). "Machine learning: Trends, perspectives, and prospects". In: *Science* 349.6245, pp. 255–260. ISSN: 0036-8075. DOI: 10.1126/science.aaa8415. eprint: http://science.sciencemag.org/content/349/6245/255.full.pdf. URL: http://science.sciencemag.org/content/349/6245/255.

Khan, T. et al. (2014). "A computer vision framework for finger-tapping evaluation in Parkinson's disease". In: *Artificial Intelligence in Medicine* 60.1, pp. 27–40. DOI:

10.1016/j.artmed.2013.11.004. URL: http://dx.doi.org/10.1016/j.artmed.2013.11.004.

Kumar, D. et al. (2015). "An Adaptive Method of PCA for Minimization of Classification Error Using Naïve Bayes Classifier". In: *Procedia Computer Science* 70. Proceedings of the 4th International Conference on Eco-friendly Computing and Communication Systems, pp. 9–15. ISSN: 1877-0509. DOI: https://doi.org/10.1016/j.procs.2015.10.018. URL: http://www.sciencedirect.com/science/article/pii/S1877050915031828.

Lainscsek, C. et al. (2012). "Finger tapping movements of Parkinson's disease patients automatically rated using nonlinear delay differential equations". In: *Chaos: An Interdisciplinary Journal of Nonlinear Science* 22.1, p. 013119. DOI: 10.1063/1.3683444. eprint: https://doi.org/10.1063/1.3683444. URL: https://doi.org/10.1063/1.3683444.

Lancet, The (2017). "Artificial intelligence in health care: within touching distance". In: *The Lancet* 390.10114, p. 2739. ISSN: 0140-6736. DOI: https://doi.org/10.1016/S0140-6736(17)31540-4. URL: http://www.sciencedirect.com/science/article/pii/S0140673617315404.

Li, M.H. et al. (2017). "Vision-Based Assessment of Parkinsonism and Levodopa-Induced Dyskinesia with Deep Learning Pose Estimation". In: *CoRR* abs/1707.09416. arXiv: 1707.09416. URL: http://arxiv.org/abs/1707.09416.

Li, Y. and Yeh, C. (2013). "Some Equivalent Forms of Bernoulli's Inequality: A Survey". In: *Applied Mathematics* 4.7, pp. 1070–1093. DOI: 10.4236/am.2013.47146. URL: https://doi.org/10.4236/am.2013.47146.

Lima, E. and Cohen, L. (1998). "Time-frequency analysis of harmonic oscillator motion". In: *Proceedings of the IEEE-SP International Symposium on Time-Frequency and Time-Scale Analysis (Cat. No.98TH8380)*, pp. 25–28. DOI: 10.1109/TFSA.1998.721352.

Liu, H. et al. (2009). "Evidence from intrinsic activity that asymmetry of the human brain is controlled by multiple factors". In: 106, pp. 20499–503.

Martinez-Manzanera, O. et al. (2016). "A Method for Automatic and Objective Scoring of Bradykinesia Using Orientation Sensors and Classification Algorithms". In: *IEEE Transactions on Biomedical Engineering* 63.5, pp. 1016–1024. ISSN: 0018-9294. DOI: 10.1109/TBME.2015.2480242.

Mathur, A. and Foody, G.M. (2008). "Multiclass and Binary SVM Classification: Implications for Training and Classification Users". In: *IEEE Geoscience and Remote Sensing Letters* 5.2, pp. 241–245. ISSN: 1545-598X. DOI: 10.1109/LGRS.2008.915597.

Medeiros, L. et al. (2016). "A Gait Analysis Approach to Track Parkinson's Disease Evolution Using Principal Component Analysis". In: *2016 IEEE 29th International Symposium on Computer-Based Medical Systems (CBMS)*, pp. 48–53. DOI: 10.1109/CBMS.2016.14.

Michell, A. W. et al. (2004). "Biomarkers and Parkinson's disease". In: *Brain* 127.8, pp. 1693–1705. DOI: 10.1093/brain/awh198. eprint: /oup/backfile/content_public/journal/brain/127/8/10.1093/brain/awh198/2/awh198.pdf. URL: http://dx.doi.org/10.1093/brain/awh198.

Miller, D.B. and O'Callaghan, J.P. (2015). "Biomarkers of Parkinson's disease: Present and future". In: *Metabolism: clinical and experimental* 64.3 0 1, S40–S46. DOI: 10.1016/j.metabol.2014.10.030. URL: https://doi.org/10.1016/j.metabol.2014.10.030.

Mitchell, T.M. (1997). *Machine Learning*. 1st ed. New York, NY, USA: McGraw-Hill, Inc. ISBN: 0070428077, 9780070428072.

Nelson-Wong, E. et al. (2009). "Application of Autocorrelation and Cross-correlation Analyses in Human Movement and Rehabilitation Research". In: *Journal of Orthopaedic & Sports Physical Therapy* 39.4. PMID: 19346626, pp. 287–295. DOI: 10.2519/jospt.2009.2969. eprint: https://doi.org/10.2519/jospt.2009.2969. URL: https://doi.org/10.2519/jospt.2009.2969.

Novotny, M. and Sedlacek, M. (2008). "RMS value measurement based on classical and modified digital signal processing algorithms". In: *Measurement* 41.3. Innovative Design and Paradigms in Instrumentation and Measurements, pp. 236–250.

ISSN: 0263-2241. DOI: https://doi.org/10.1016/j.measurement.2006.11.011. URL: http://www.sciencedirect.com/science/article/pii/S0263224106002399.

OpenPose (2017a). *Hand Output Format*. URL: https://raw.githubusercontent.com/CMU-Perceptual-Computing-Lab/openpose/master/doc/media/keypoints_hand.png (visited on 08/08/2018).

– (2017b). *Pose Output Format (COCO)*. URL: https://raw.githubusercontent.com/CMU-Perceptual-Computing-Lab/openpose/master/doc/media/keypoints_pose_18.png (visited on 08/08/2018).

Pal, G. and Goetz, C. (2013). "Assessing Bradykinesia in Parkinsonian Disorders". In: *Frontiers in Neurology* 4.54, pp. 1–5. ISSN: 1664-2295. DOI: 10.3389/fneur.2013.00054. URL: https://www.frontiersin.org/article/10.3389/fneur.2013.00054.

Paradis, Emmanuel (2009). "Moran ' s Autocorrelation Coefficient in Comparative Methods". In:

Parkinson's Foundation (2018a). *Stages of Parkinson's*. URL: http://www.parkinson.org/Understanding-Parkinsons/What-is-Parkinsons/Stages-of-Parkinsons (visited on 07/27/2018).

– (2018b). *Statistics*. URL: http://parkinson.org/Understanding-Parkinsons/Causes-and-Statistics/Statistics (visited on 07/28/2018).

Parkinson's Progression Markers Initiative (2018). *A LANDMARK STUDY OF PARKINSON'S DISEASE*. URL: http://www.ppmi-info.org/ (visited on 07/28/2018).

Pedregosa, F. et al. (2011). "Scikit-learn: Machine Learning in Python". In: *Journal of Machine Learning Research* 12, pp. 2825–2830.

Pownuk, A. and Kreinovich, V. (2017). *Why Linear Interpolation?* Departmental Technical Reports (CS).

Rafiee, J. and Tse, P.W. (2009). "Use of autocorrelation of wavelet coefficients for fault diagnosis". In: *Mechanical Systems and Signal Processing* 23.5, pp. 1554–1572. ISSN: 0888-3270. DOI: https://doi.org/10.1016/j.ymssp.2009.02.008. URL: http://www.sciencedirect.com/science/article/pii/S0888327009000685.

Raschka, S. and Mirjalili, V. (2017). *Python Machine Learning, 2nd Ed.* 2nd ed. Birmingham, UK: Packt Publishing. ISBN: 978-1787125933.

Saito, Takaya and Rehmsmeier, Marc (2015). "The Precision-Recall Plot Is More Informative than the ROC Plot When Evaluating Binary Classifiers on Imbalanced Datasets". In: *PLOS ONE* 10.3, pp. 1–21. DOI: 10.1371/journal.pone.0118432. URL: https://doi.org/10.1371/journal.pone.0118432.

Sanborn, S. and Ma, X. (2005). "Quantifying information content in data compression using the autocorrelation function". In: *IEEE Signal Processing Letters* 12.3, pp. 230–233. ISSN: 1070-9908.

Saravanan, T.J., Gopalakrishnan, N., and Rao, N.P. (2015). "Damage detection in structural element through propagating waves using radially weighted and factored RMS". In: *Measurement* 73, pp. 520–538. ISSN: 0263-2241. DOI: https://doi.org/10.1016/j.measurement.2015.06.015. URL: http://www.sciencedirect.com/science/article/pii/S0263224115003292.

Schlossmacher, M. and Mollenhauer, B. (2010). "Biomarker research in Parkinson's disease: objective measures needed for patient stratification in future cause-directed trials". In: *Biomarkers in Medicine* 4.5, pp. 647–650. DOI: 10.2217/bmm.10.93. eprint: https://doi.org/10.2217/bmm.10.93. URL: https://doi.org/10.2217/bmm.10.93.

Sharma, S. et al. (2013). "Biomarkers in Parkinson's disease (recent update)". In: *Neurochemistry International* 63.3, pp. 201–229. DOI: https://doi.org/10.1016/j.neuint.2013.06.005. URL: http://www.sciencedirect.com/science/article/pii/S0197018613001678.

Shi, J., Liu, J., and Qu, Q. (2014). "Handedness and dominant side of symptoms in Parkinson's disease". In: *Medicina Clínica* 142.4, pp. 141–144. ISSN: 0025-7753. DOI: https://doi.org/10.1016/j.medcli.2012.11.028. URL: http://www.sciencedirect.com/science/article/pii/S0025775312009803.

SILSO World Data Center. "The International Sunspot Number". In: *International Sunspot Number Monthly Bulletin and online catalogue.*

Simon, Tomas et al. (2017). "Hand Keypoint Detection in Single Images using Multiview Bootstrapping". In: *CVPR*.

Simpson, J.R. and Montgomery, D.C. (1998). "A robust regression technique using compound estimation". In: *Naval Research Logistics (NRL)* 45.2, pp. 125–139. DOI: 10.1002/(SICI)1520-6750(199803)45:2<125::AID-NAV1>3.0.CO;2-A. URL: https://onlinelibrary.wiley.com/doi/abs/10.1002/%28SICI%291520-6750%28199803%2945%3A2%3C125%3A%3AAID-NAV1%3E3.0.CO%3B2-A.

The Michael J. Fox Foundation (2018). *Deep Brain Stimulation*. URL: https://www.michaeljfox.org/understanding-parkinsons/living-with-pd/topic.php?deep-brain-stimulation (visited on 07/30/2018).

Ťupa, Ondřej et al. (2015). "Motion tracking and gait feature estimation for recognising Parkinson's disease using MS Kinect". In: *BioMedical Engineering OnLine* 14.1, p. 97. ISSN: 1475-925X. DOI: 10.1186/s12938-015-0092-7. URL: https://doi.org/10.1186/s12938-015-0092-7.

Tysnes, O.B. and Storstein, A (2017). "Epidemiology of Parkinson's disease". In: *Journal of Neural Transmission* 124.8, pp. 901–905. ISSN: 1435-1463. DOI: 10.1007/s00702-017-1686-y. URL: https://doi.org/10.1007/s00702-017-1686-y.

Urbanowski, Krzysztof (2017). "True quantum face of the "exponential" decay law". In: *The European Physical Journal D* 71.118, pp. 1–6. ISSN: 1434-6079. DOI: 10.1140/epjd/e2017-70666-0. URL: https://doi.org/10.1140/epjd/e2017-70666-0.

van der Hoorn, A. et al. (2011). "Handedness and dominant side of symptoms in Parkinson's disease". In: *Parkinsonism & related disorders* 17, pp. 58–60. DOI: 10.1016/j.parkreldis.2010.10.002.

Wang, Z. and Bovik, A. C. (2009). "Mean squared error: Love it or leave it? A new look at Signal Fidelity Measures". In: *IEEE Signal Processing Magazine* 26.1, pp. 98–117. ISSN: 1053-5888. DOI: 10.1109/MSP.2008.930649.

Wei, Shih-En et al. (2016). "Convolutional pose machines". In: *CVPR*.

Wittke, P. (1964). "The autocorrelation function of the output of a nonlinear angle modulator". In: *IEEE Transactions on Information Theory* 10.1, pp. 67–72. ISSN: 0018-9448. DOI: 10.1109/TIT.1964.1053645.

Wong, C. et al. (2015). "Wearable Sensing for Solid Biomechanics: A Review". In: *IEEE Sensors Journal* 15.5, pp. 2747–2760. ISSN: 1530-437X. DOI: 10.1109/JSEN.2015.2393883.

Wu, Z. et al. (2007). "On the trend, detrending, and variability of nonlinear and nonstationary time series". In: *Proceedings of the National Academy of Sciences* 104.38, pp. 14889–14894. ISSN: 0027-8424. DOI: 10.1073/pnas.0701020104. eprint: http://www.pnas.org/content/104/38/14889.full.pdf. URL: http://www.pnas.org/content/104/38/14889.

Zhou, Z. (2014). "Measuring nonlinear dependence in time-series, a distance correlation approach". In: *Journal of Time Series Analysis* 33.3, pp. 438–457. DOI: 10.1111/j.1467-9892.2011.00780.x. URL: https://onlinelibrary.wiley.com/doi/abs/10.1111/j.1467-9892.2011.00780.x.